SLAC-PUB-2849
November 1981
(E/A)

LINEAR COLLIDER*

A Preview

by

H. Wiedemann
Stanford Linear Accelerator Center
Stanford University, Stanford, California 94305

Lecture given at the 1981 Summer School on Particle Physics, Stanford Linear Accelerator Center, July 27-August 7, 1981

* Work supported by the Department of Energy, contract DE-AC03-76SF00515.

Table of Contents

GENERAL INTRODUCTION

In the past decade progress in high energy physics was largely dominated by experimental results obtained in electron-positron colliding beam storage rings. This progress underlines the maturity of the technique which allows the confident proposal of new storage rings with ever increasing center-of-mass energies. While there does not seem to be a fundamental limit to the principle below a center-of-mass energy of about 500 GeV,[1] it seems that we have reached the fiscal limit with the proposed e^+e^- storage ring, LEP, at CERN, Geneva.[2] This storage ring has a circumference of 28 km and is supposed to reach a center-of-mass energy of 160 GeV with a conventional RF system and 240 GeV with a superconducting RF system when this technique becomes practical. The version with the conventional RF system is estimated at about $600M plus the cost of personnel. The different generations of storage rings built and estimated so far lead us to a scaling of the cost with the square of the energy. This comes from the rapidly increasing demand for RF power with energy to compensate the losses due to synchrotron radiation in the circular ring magnets. In order to keep this power demand and the energyspread in the beam reasonable, the designer is forced to increase the circumference of the storage ring at least like the square of the energy. It is clear that the scaling for cost and size makes the proposal of a storage ring with significantly higher energy than LEP unrealistic. An alternative for colliding beam facilities are Linear Colliders.[3] Here two linear accelerators, one for positrons and one for electrons, face each other. Both linear accelerators are triggered at the same time and the beams are brought into head-on collision at the interaction point in the same manner as in a storage ring. This way no bending of the beams is involved and as a consequence there is no energy loss due to synchrotron radiation.

The cost scaling, therefore, must go linear with the energy. Since no linear colliders have been built yet it is difficult to know at what energy the linear cost scaling of linear colliders drops below the quadratic scaling of storage rings. There is, however, no doubt that a linear collider facility for a center of mass energy above say 500 GeV is significantly cheaper than an equivalent storage ring.

In order to make the linear collider principle feasible at very high energies a number of problems have to be solved. There are two kinds of problems: One which is related to the feasibility of the principle and the other kind of problems is associated with minimizing the cost of constructing and operating such a facility.

In this lecture series I will try to describe the problems and possible solutions. Since the real test of a principle requires the construction of a prototype I will in the last chapter describe the SLC project at the Stanford Linear Accelerator Center.

1. BASIC PROCESSES AND COMPONENT

In a linear collider facility two linear accelerators aimed at each other on a straight line are fired at the same time (Fig. 1). Both beams are brought into head-on collision at the collision point halfway between both linear accelerators. If one accelerator produces a bunch of electrons and the other a bunch of positrons we have e^+e^- collisions like in a storage ring. The luminosity is given by

$$\mathcal{L}_c = \frac{N^2 \nu_{rep}}{4\pi \sigma_x^* \sigma_y^*} \qquad (1.1)$$

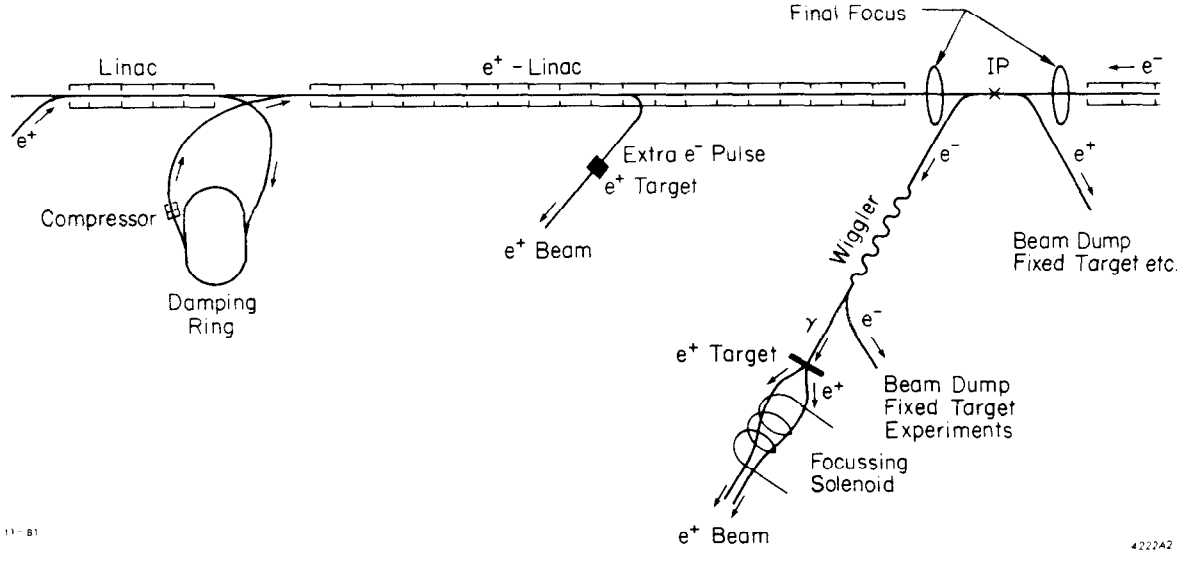

Fig. 1: Schematic Layout of a Colliding Beam Facility

where $N^+ = N^- = N$ is the number of particles per bunch, ν_{rep} the pulse repetition rate and, σ_y^* the beam height at the collision point. From here on all quantities shown with an asterix (σ_y^*, etc.) are to be taken at the collision point. To bring the luminosity expectations into perspective we have to compare it with a storage ring luminosity given by

$$\mathscr{L}_s = \frac{B_s N_s^2 \nu_{rev}}{4\pi \sigma_x^* \sigma_y^*} \tag{1.2}$$

where ν_{rev} is the revolution frequency and B_s the number of bunches per beam. We are being a little generous in assuming $\mathscr{L}_s \sim B_s$ because that proportionality was never quite achieved in a real storage ring due to the beam beam effect.[4)]

We now take the ratio of both luminosities and apply subscripts "c" and "s" for collider and storage ring respectively to the beam quantities and set $B_c = 1$:

$$\frac{\mathscr{L}_c}{\mathscr{L}_s} = \frac{1}{B_s} \frac{N_c^2}{N_s^2} \frac{\nu_{rep}}{\nu_{rev}} \frac{\sigma_{sx}^* \sigma_{sy}^*}{\sigma_{cx}^* \sigma_{cy}^*} \tag{1.3}$$

For fiscal reasons we will always have to choose $\nu_{rep} << \nu_{rev}$ and limitations due to the interaction of the beam with the accelerator structure will require the number of particles per bunch to be much smaller in the collider than in a storage ring, $N_c << N_s$. In order to still achieve collider luminosities comparable with storage ring luminosities we have to make the beam cross section of the collider beams at the collision point extremely small, $\sigma_{cx}^*, \sigma_{cy}^* << \sigma_{sx}^*, \sigma_{sy}^*$. This is possible in a linear collider facility. In a storage ring the lower limit of the beam cross section is determined by the beam beam effect and the limitations in our ability to correct chromatic effects

in the focussing system. These limitations arise because the particles may not be perturbed too much by the beam beam effect so they can be used again and again as they circulate in the storage ring. In a linear collider the particles are thrown away after collision and, therefore, we can make the beam cross section as small as technically feasible.

To maximize the luminosity in a linear collider we, therefore, need:

- the highest number of electrons and positrons per bunch that can safely be accelerated without getting a dilution of the beam emittance.
- the smallest possible beam emittance ε, since $\sigma^* = \sqrt{\varepsilon\beta^*}$,
- the tighest possible focussing at the collision point (small β^*),
- the highest technically and financially feasible pulse repetition rate (ν_{rep}).

Now we are ready to understand the basic processes taking place in each cycle of the linear collider system (see Fig. 1).

- an intense bunch of electrons in a short pulse compatible with the wavelength of the linear accelerator is generated and injected into the accelerating structure.
- at about the same time an intense positron bunch is created and also at an appropriate phase injected into the other accelerating structure.
- since neither the electron nor the positron bunch have the desired small beam emittance both bunches after some acceleration to the order of about 1 GeV are stored in so-called damping rings. These rings are small storage rings where the particles reduce their transverse momentum (beam emittance) due to the emission of synchrotron radiation.
- after a few damping times the electron and positron bunches are ejected from the damping ring again and accelerated to the final energy in the linear

accelerators.

- during acceleration a sophisticated monitoring and control system is used to keep the beams as close as possible in the center of the accelerating structure. This is necessary to minimize the excitation of transverse electromagnetic modes (wake fields) which act back on the beams in a destructive way (Section 6).
- after acceleration the beams are transported through a final focus system which focusses the beam dimension to as small a diameter at the collision point as possible. The limitation is determined only by the chromatic and geometric aberrations of the beam optical focussing system (Section 7).
- after the beams have collided they have to be disposed of properly in a beam dump or they may be used for fixed target experiments. In either case, the beams could first create high energy γ's in a wiggler magnet which then are used to produce the positrons for the next cycle (Fig. 1)(Section 5).

A more detailed discussion of major components will follow in subsequent sections of these lectures. The damping ring complex, however, we will discuss here since we need its scaling laws in the next section.

1.1 Damping Ring

The damping ring complex consists of three parts: the damping ring, the bunch length compressor to match the long bunch from the damping ring to the short bunch in the linac, and spin rotation elements.

Electrons and more so positrons are produced with a beam emittance much larger than required for use in linear colliders. Therefore, it is necessary to "cool" the beams in specially designed storage rings. The cooling is achieved by the synchrotron radiation and the way the lost energy is replenished by the RF accelerating system. Particles radiate photons along their trajectories and, therefore, experience a loss in transverse momentum.

In the accelerating cavity, however, the lost momentum is replaced only along the longitudinal axis. Therefore, the net effect on the particle due to photon emission and RF acceleration is a reduction in transverse momentum or a damping of the transverse beam size. There is also, however, an excitation effect due to the quantized emission of photons. This causes a sudden change in the energy of the particle which in turn together with the focussing properties of the lattice causes quantum fluctuations of the transverse oscillation amplitudes and, therefore, an increase in beam size[5]. Both damping and quantum excitation lead to an equilibrium beam size. By proper choice of the storage ring parameters the beam size or beam emittance can be made very small. The evolution of the normalized beam emittance during damping is given by

$$\psi = \psi_D(1 - e^{-2n}) + \psi_o\, e^{-2n} \tag{1.4}$$

where $\psi = \varepsilon\gamma$, ε the beam emittance, ψ_D the equilibrium beam emittance, ψ_o the emittance of the injected beam and n the number of damping times the beam is damped in the storage ring. In general, we want very "cool" beams at a high repetition rate. This means we have to use high bending magnet fields for fast damping and high quadrupole field gradients to reduce the effect of quantum excitation on the beam emittance. Under certain general assumptions scaling laws for the damping ring parameters can be derived which are independent of the linear collider parameters.[6] The resulting parameters all can be expressed in terms of $\nu_{rep}/N_B N_s$ where ν_{rep} is the desired linac pulse repetition rate, N_B the number of bunches to be damped at any one time in each damping ring and N_s the number of active damping rings for each kind of beam. In Fig. 2 the energy E_D, the bending radius ρ_D, the magnet length L_m and the normalized beam emittance ψ_D are shown. These parameters

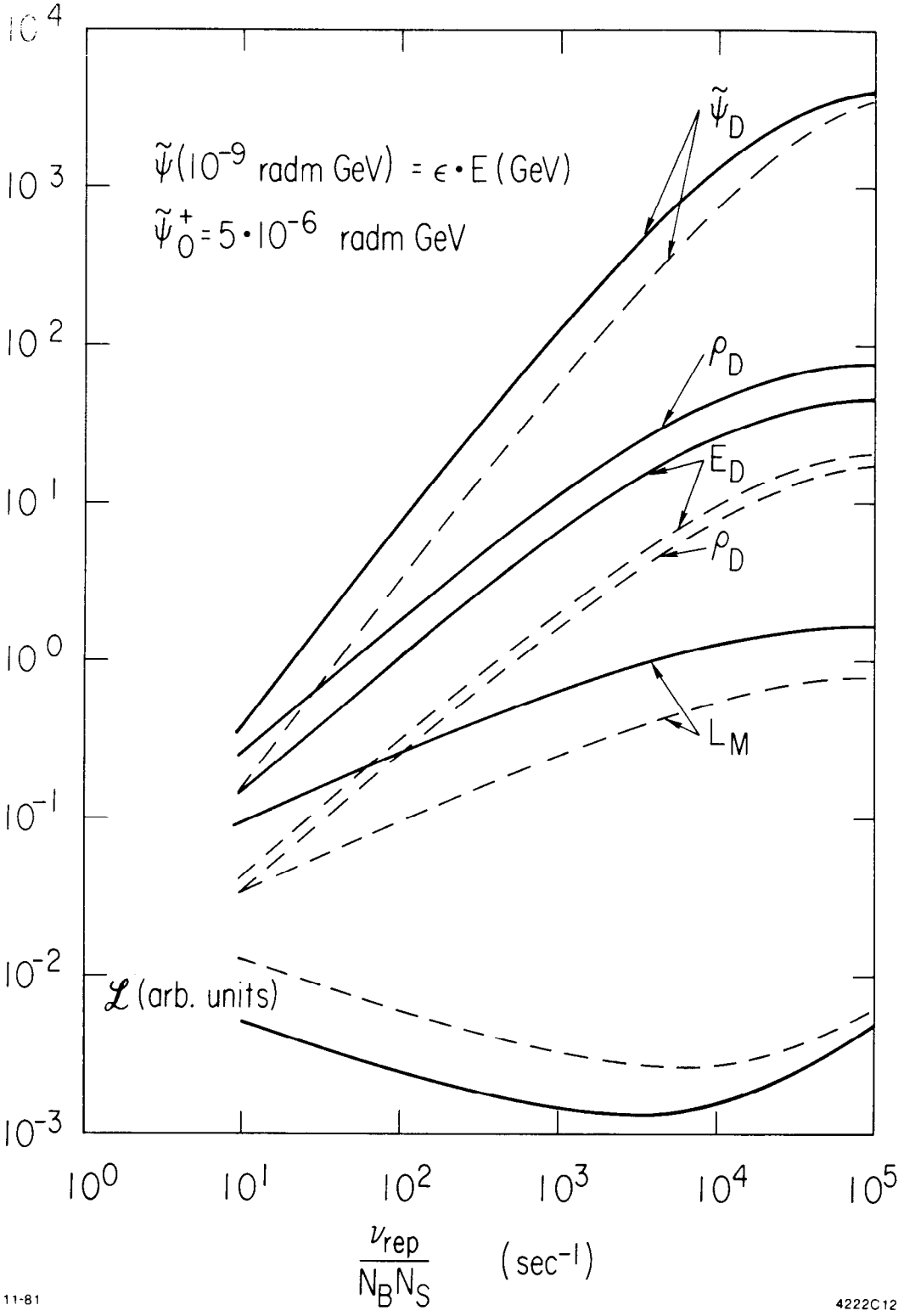

Fig. 2: Damping Ring Scaling

will be important when we discuss possible parameters for linear colliders at very high energies. The solid lines in Fig. 2 are given for conventional magnets (B = 20 kG, g = 10 kG/cm) and the dotted lines are for superconducting magnets (B = 40 kG, g = 20 kG/cm). The influence of the damping ring parameters on the luminosity ($\mathscr{L} \sim \nu_{rep}/\varepsilon$) is also shown in Fig. 2.

We observe in Fig. 2 that for high repetition rates the energy of the damping ring is rather large while the benefits are small. At very high repetition rates we actually reach a point where even with a powerful damping ring the beam emittance cannot be reduced below the emittance of the positrons coming from a positron target or in other words, at these repetition rates and above we do not need a damping ring anymore. Here we have assumed an emittance of the positron source as designed for the SLC[7] which seems to be close to technical limits. At very low repetition rates we reach a technical limit since all components get too small. However, considering the dependence of luminosity and of the operating costs on the repetition rate it is clear that the lowest possible rate should be chosen. For conventional magnets values of $(\nu_{rep}/N_B N_s)_{min}$ = 50 to 100 sec^{-1} seem to be technically feasible.

1.2 Bunch Length Compressor

The beam as delivered by the damping ring cannot properly be accelerated in a linear accelerator since the bunchlength is long compared with the RF wavelength of an S-band linac which would lead to a large energy spread in the beam. We, therefore, have to send the beams through a bunch length compression system. This system consists of two parts. The first part is a RF cavity which is phased such that the center of the bunch does not see any field. We also require the RF phase to be such that the particles ahead of the center see an accelerating field and the particles behind the center see a decelerating field. After the beam has passed this cavity the particles

ahead of the center all have higher energies and particles behind the center all have lower energies than the central particle. Now we let this beam go through a non-isochronous beam transport system which is designed such that a particle with higher energy will travel a lower path than a particle with lower energy. If the parameters of this transport system are correctly chosen at the entrance to the linac the bunch will just have shrunk to its minimum size.

To follow the process more quantitatively we assume the energy spread and the bunchlength of the beam as it comes out of the damping ring to be $\sigma_{\varepsilon o}/E$ and $\sigma_{\ell o}$, respectively (Fig. 3). If s is the longitudinal distance of a particle from the bunch center (s > 0 for the head of the bunch) then a particle going through the compressor cavity gains an energy of

$$\varepsilon = \frac{2\pi}{\lambda_{rf}} \hat{V}_{rf} \cdot s \tag{1.5}$$

where $V_{rf} = \hat{V}_{rf} \sin \phi$, λ_{rf} the RF wavelength, and $\sin \phi \approx \phi$ or $\sigma_{\ell o} << \lambda_{rf}$. As the beam travels through the non-isochronous transport line every particle changes its position s according to

$$\Delta s = - F_c \frac{\varepsilon}{E} \tag{1.6}$$

where F_c is the compression factor of the transport line and depends only on the parameters of this line. Since we want a particle originally at position s to move to the center of the beam we have from Eq. (1.5) and Eq. (1.6)

$$s + \Delta s = 0 = s - F_c \frac{2\pi}{\lambda_{rf}} \frac{\hat{V}_{rf}}{E} s \tag{1.7}$$

or if we solve for the RF-voltage:

$$\hat{V}_{rf} = \frac{\lambda_{rf}}{2\pi} \frac{E}{F_c} \tag{1.8}$$

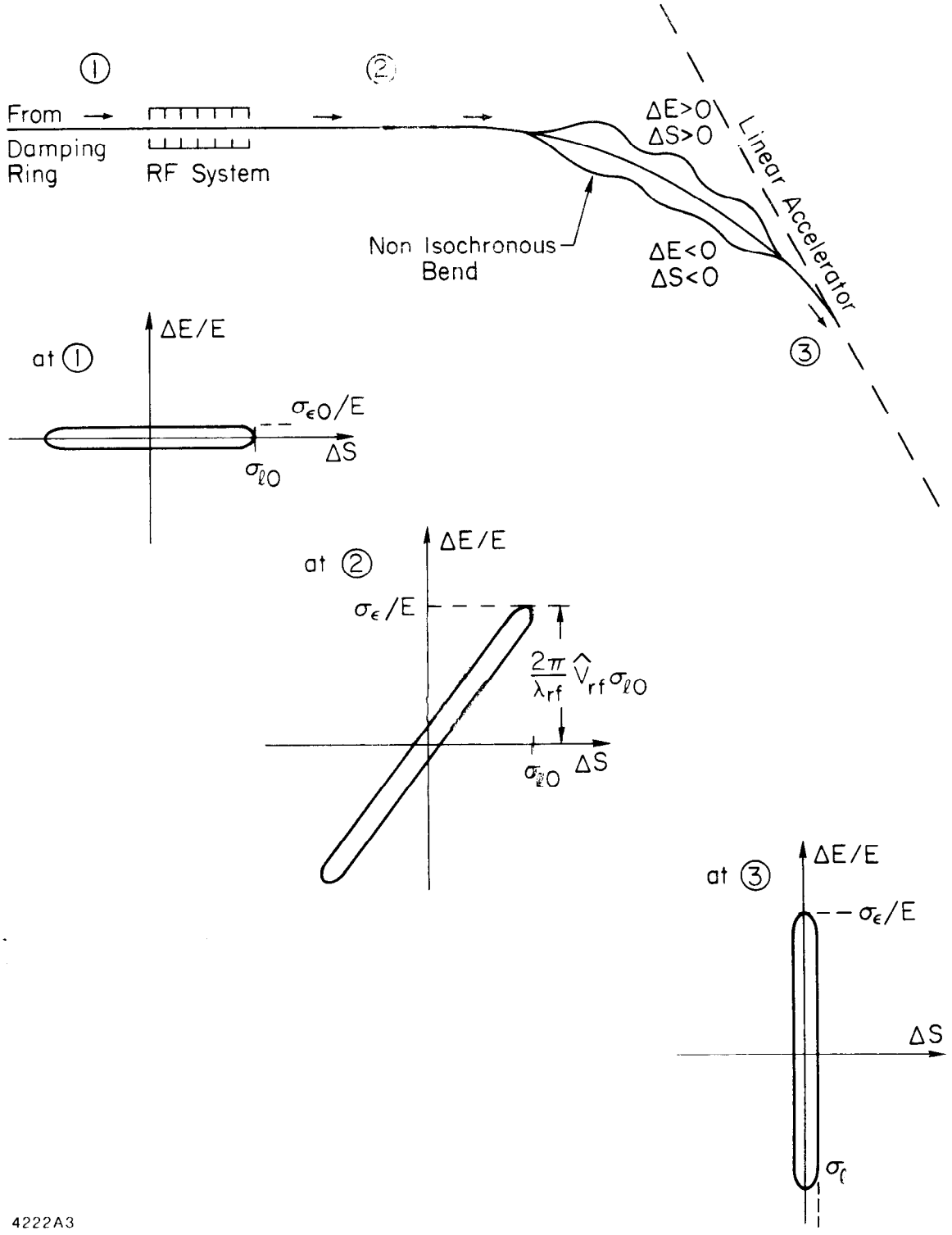

Fig. 3: Bunch Length Compressor

The required RF voltage is independent of the bunchlength as is easily recognized from Fig. 3. This, however, is true only as long as we can set $\sin \phi \approx \phi$ over the bunchlength.

Because of the finite distribution of the beam in the $\varepsilon - \phi$ phase space we cannot make the bunchlength to collapse to zero. The area of the beam in phase space is conserved or $\sigma_{\varepsilon o} \cdot \sigma_{\ell o} = \sigma_\varepsilon \sigma_\ell$ where σ_ε, σ_ℓ are the energy spread and bunchlength at the linac. If we applys Eqs (1.5) to (1.8) to a finite phase ellipse (Fig. 3) we get

$$\sigma_\ell = F_c \frac{\sigma_{\varepsilon o}}{E} \tag{1.9}$$

and

$$\frac{\sigma_\varepsilon}{E} = \frac{\sigma_{\ell o}}{F_c} \tag{1.10}$$

The significant result of this bunch compression scheme is that the shorter bunchlength is achieved only at the cost of a much larger energy spread and the chromatic effects in the transport line have to be corrected.

1.3 Spin Rotators

The damping ring complex has one more important component - the spin manipulation devices. The knowledge of the polarization of the colliding electrons and positrons will be more and more important for the experimental program at the very high energies of linear colliders. In Section 5 we will discuss methods to produce longitudinally polarized electron and positron beams. At the collision point we would like to have total freedom in the choice of the polarization of either beam: longitudinal, transverse or no polarization. This requires some spin manipulation devices. Since all beams have to pass through the damping ring we have to take special care to align the spin with the vertical bending field in the

damping ring in order not to destroy the polarization. To be able to rotate the spin in any direction we need transverse and longitudinal magnetic fields. In Section 5 we will discuss more details of these spin rotators.

2. Scaling Laws

In order to optimize a linear colliding beam facility or at least to find the problem areas we need to know the scaling laws of such a facility.

The luminosity is given by

$$\mathscr{L}_o = \frac{N^2 \nu_{rep}}{4\pi\sigma^{*2} R} \tag{2.1}$$

where $\mathscr{L}_o$ is the luminosity without pinch effect, $\sigma^* = \sigma_y^*$ and $R = \sigma_x^*/\sigma_y^*$ at the collision point.

As the beams penetrate each other every particle is exposed to the electromagnetic field of the other beam. This field deflects the trajectory of the particle and the particle in turn emits synchrotron radiation which we call "breamstrahlung".[1] This beamstrahlung increases the energy spread in the beam but since we do not want this energy spread to become too large we have to include this phenomenon in our scaling laws. The average energy lost by a particle in a transverse magnetic field of length δs is $\delta E = C_\gamma E^4/\rho \cdot \delta s/2\pi\rho$ where $C_\gamma = 4\pi r_e/3(mc^2)^3$ and ρ the bending radius in the electromagnetic field. The total energy loss of a particle after the beams have collided then is given by:

$$\frac{\Delta E}{E} = \frac{2\, r_e}{3}\, \gamma^3 \int \frac{ds}{\rho^2(s)} \tag{2.2}$$

The integral has been evaluated for a Gaussian beam:[8)]

$$\int \frac{ds}{\rho^2(s)} = \frac{r_e^{\,2}\, N^2}{\gamma^2\, \sigma^{*2}_R\, \sigma_\ell} \underbrace{\frac{4}{\sqrt{\pi}} \frac{1}{R\sqrt{P}} \begin{cases} 2 \arctan\left(\sqrt{P/Q}\right) & \text{for } P > 0 \\ \ell n\, \dfrac{1 + \sqrt{P/Q}}{1 - \sqrt{P/Q}} & \text{for } P < 0 \end{cases}}_{F(R)} \tag{2.3}$$

where $P = 3/R^4 - 10/R^2 + 3$ and $Q = 3/R^2 + 8/R + 3$. We, therefore, have as a scaling law

$$\frac{\Delta E}{E} = \frac{2\, r_e^{\,3}}{3}\, \frac{N^2}{\sigma^{*2}_R\, \sigma_\ell}\, \gamma \cdot F(R) \tag{2.4}$$

with $F(1) = 0.325$ and $F(R \gg 1) \approx 1.3/R$

At this point it should be noted that Eq. (2.4) is true only if the bunches keep their transverse distribution while they collide. Later we will see that the luminosity is significantly increased if we create a situation where the bunches focus each other creating a pinch effect. In this case, the energy spread due to beamstrahlung is changed and has to be calculated numerically. For scaling we will, however, use Eq. (2.4).

The next quantity we would like to control is the so-called disruption parameter. Each beam acts on every particle of the other beam as they collide like a focussing quadrupole magnet. The deflection of the trajectories have given rise to synchrotron radiation as described in the last paragraph. However, the focussing can also reduce the beam cross section (pinch effect) thus enhancing the particle density and the luminosity. This will be discussed in more detail in Section 7. The luminosity enhancement factor due to the pinch effect depends on the value of the disruption parameter D and reaches a maximum value for $D \approx 4$. The disruption parameter D is defined by $D = \sigma_\ell / f$ where σ_ℓ is the bunchlength and f is the focal length of the electromagnetic field in the center part of the beam. In more convenient parameters we have

$$D = \frac{2 r_e N \sigma_\ell}{\gamma \sigma^{*2} (1 + R)} \tag{2.5}$$

The disruption parameter is closely related to the linear beam beam tune shift, $\Delta\nu_s$, in a storage ring

$$\Delta\nu_s = \frac{\beta_s^*}{4\pi\sigma_\ell} D \tag{2.6}$$

where β_s^* is the betatron function[9] at the interaction point of the storage ring.

In the following we assume certain quantities to be fixed a priori either by design or technical limitations and other parameters will be a consequence of these assumptions. Certainly, there is a large amount of freedom in the choice of these fixed parameters. We will use as input parameters the luminosity, $\mathscr{L}_o$, the maximum energy spread due to beamstrahlung that we want to tolerate, the bunch length σ_ℓ as determined by the frequency of the linear accelerator, the value β^* of the betatron function at the interaction point which is limited by chromatic and geometric errors in the final focus system, the disruption parameter D to gain an additional factor in luminosity and the beam aspect ratio R as a free parameter.

From Eqs.(2.4) and (2.5) we then get for the beam size σ^* and normalized beam emittance $\psi = \varepsilon\gamma$ where $\varepsilon = \sigma^{*2}/\beta^*$

$$\sigma^{*2} = \frac{6}{r_e}\frac{\sigma_\ell^3}{\gamma^3}\frac{\Delta E/E}{D^2}\frac{R}{(1+R)^2F(R)} \tag{2.7}$$

or

$$\psi = \frac{6}{r_e}\frac{\sigma_\ell^3}{\gamma^2}\frac{\Delta E/E}{D^2\beta^*}\frac{R}{(1+R)^2F(R)} \tag{2.8}$$

From Eqs. (2.6) and (2.4) we get for the number of particles per bunch

$$N = \frac{3}{r_e^2}\frac{\sigma_\ell^2}{\gamma^2}\frac{\Delta E/E}{D}\frac{R}{(1+R)\,F(R)} \tag{2.9}$$

From Eqs. (2.1) and (2.7) and (2.9) we get for the pulse repetition rate ν_{rep}:

$$\nu_{rep} = \frac{8\pi}{3}r_e^3\frac{\gamma\,\mathscr{L}_o}{\sigma_\ell\,(\Delta E/E)}\,F(R) \tag{2.10}$$

Last but not least we get for the beam power from $P_B = N \cdot E \cdot \nu_{rep}$ and using Eqs. (2.9) and (2.10).

$$P_B = (8\pi\, r_e\, mc^2)\, \frac{\sigma_\ell\, \mathcal{L}_o}{D}\, \frac{R}{1+R} \qquad (2.11)$$

It is obvious from Eqs. (2.10) and (2.11) that the electric power required to run a linear collider is just proportional to the luminosity. Since the beam takes only a few percent of the energy from the accelerating cavities one should concentrate on Eq. (2.10) to reduce the total power consumption which is proportional to the repetition rate. From this equation we see that the bunchlength σ_ℓ should be large, the energy spread due to beamstrahlung big and the beam should be flat $R >> 1$. As for the bunchlength we have to consider the linac frequency. Since the accelerating field is not uniform along the bunch one should choose a short bunch in order to minimize the energy spread in the beam. A compromise between power consumption and energy spread has to be established for every particular accelerating field distribution in phase. We also find that a large aspect ratio R should be chosen. This is not difficult to achieve but at the same time the required number of particles per bunch increases ($N \sim R$ for $R >> 1$) and we may face problems connected with the interaction of the bunch with the cavities of the accelerating structure creating so-called "wakefields" which can destroy the beam emittance. Ultimately, therefore, the optimum aspect ratio R will be determined by limitations due to wake field effects. Where the number of particles per bunch is of no concern one might also increase the allowable energy spread $\Delta E/E$ to reduce the power consumption. The limit here might be given by experimental reasons or by limitations in the ability to correct chromatic aberrations in the final focus system.

Using these scaling laws we derive a set of parameters (Table 2.1) for a linear collider facility using certain assumptions for the free parameters. This model we will use in the discussions of the next sections to develop a feeling for the order of magnitudes of significant design parameters. In Section 4 we will try to sketch an optimization of parameters.

Table 2.1
Design Example for a Linear Collider

Energy	$E = 2 \times 350$ GeV
Luminosity (no pinch effect)	$\mathcal{L}_o = 1 \cdot 10^{36}$ m^{-2} sec^{-1}
(with pinch effect)	$\mathcal{L} = 6 \cdot 10^{36}$ m^{-2} sec^{-1}
Aspect Ratio	$R = \sigma_x^*/\sigma_y^* = 7$
Bunchlength	$\sigma_\ell = 2$ mm
Energy spread due to Beamstrahlung	$\Delta E/E = 2\%$
Disruption Parameter	$D = 4$
Beam Size ($\beta^* = 0.01$ m)	$\sigma_x^* = 1.40$ μm
	$\sigma_y^* = 0.20$ μm
Beam Emittance	$\varepsilon_x = 2.10^{-10}$ rad m
# of Particles per Bunch	$N = 9.8 \cdot 10^{10}$
Pulse Repetition Rate	$\nu_{rep} = 460$ sec^{-1}
# of Bunches N_B times # of Damping Rings N_s	$N_B N_s = 2$
Energy of Damping Ring	$E_D = 2.2$ GeV
Beam Power of Collider	$P_B = 2 \times 2.5$ MW

The length of the facility as well as the power consumption for RF alone are very high. We notice, however, that only 0.5% of the ac-power is delivered to the beams while the rest of the energy is wasted in the accelerating structure or coupled out into an absorber.

3. SUPER HIGH ENERGY LINEAR ACCELERATOR SYSTEMS

The parameters of the linear accelerator structure used to get to hundreds of GeV per beam will have a major impact on the overall performance and cost of the facility, both for construction and operation. In order to understand the problems we will start out with known and proven techniques and will then try to identify new techniques necessary to arrive at more reasonable parameters.

We assume that we want to build a linear collider facility with a center-of-mass energy of

$$E_{cm} = 700 \text{ GeV} \tag{3.1}$$

or 350 GeV per beam.

First, we ask ourselves where do we end up if we assume a SLAC-type linac equipped with an RF-pulse compression system to get higher accelerating fields at the expense of the pulse length.[10] For this type of operation a gradient of 17 MeV/m can be achieved with 250 klystrons each delivering 38 MW for 5 μsec into a 3 m long section.[7] For a linear collider system with E_{cm} = 700 GeV we would for our design example (Table 2.1) of the previous section arrive at the parameters of Table 3.1.

Table 3.1
Length and Power Consumption for a SLAC Type Facility

E_{cm}	=	700 GeV	g	=	17 MV/m
L	=	2 x 20.6 km	ν_{rep}	=	460 sec
P_{RF}	=	2 x 150 MW			
P_{ac}	=	2 x 500 MW (klystron efficiency 30%)			
P_B	=	2 x 2.5 MW			
η	=	$2\ P_B/P_{ac}$ = 0.5%			

The large amount of dissipated energy in the structure lead people to propose superconducting structures for the accelerator.[3)11)12)] In this case there is little dissipation of energy in the structure, although at $4.2^{o}K$ or less an enormous amount of electrical power has to be spend to run refrigerating systems which have achieved an efficiency of no better than 1/400. Because of the low accelerating fields achieved so far the linac also is very long which makes the heat losses of the cryostat significant. Due to the interaction of the intense bunch with the accelerating structure an additional heat source is created in the form of higher-order-modes in the structure. These losses are very significant and it is absolutely neceseary to couple out these modes from the cavities.

To be more quantitative we calculate the RF losses from:

$$P_{rf\ disc} = \frac{g^2 \ell}{Q_o (r/Q_o)} \tag{3.2}$$

where g is the gradient and ℓ the structure length. We assume for the numerical calculations $Q_o = 1.3 \cdot 10^9$ and $r/Q_o = 2000\Omega/m$ for $\nu_{rf} = 3000$ MHz and Nb cells, values that may be disputed but compared with parameters quoted in the literature they seem to be on the optimistic side. For the heat losses of the cryostat we assume 2 W/m which is half the measured value of a 4 m RF separator.[13)14)] The factor 1/2 seems to be justified since the cryostat for a 3 GHz linac structure may be smaller than the 1 m diameter of the RF separator.

To estimate higher-order-mode losses we take the measured value for the SLAC linac which was[39)] 50 MeV for 10^9 particles in one S-band bunch and 86000 cavities or a total length of 3 km.

If we assume a similar bunch length in our superconducting linac and the same RF-frequency we can scale like

$$P_{HOM}(eV/sec) = 50 \cdot 10^6 \nu_{rep} \left(\frac{N}{10^9}\right)\left(\frac{L(m)}{3000}\right) N \qquad (3.3)$$

and we get for our design example:

$$P_{HOM}(W) = 11.8 \cdot L(m) \qquad (3.4)$$

with these assumptions the electrical power requirements are calculated and tabulated in Table 3.2 for different gradients in the superconducting structure:

Table 3.2
Length and Power Consumption for a Superconducting Linac

E_{cm} = 700 GeV

g(MV/m)	3	7	10	20
L_{tot}(km)	233	100	70	35
P_H (kW)	470	200	140	70
$P_{RF\ diss}$(kW)	809	1885	2692	5385
P_{HOM}(kW)	2749	1180	826	413
$P_{tot\ ac}$(MW)	523	839	1136	2184

Here P_H are the heat losses from the cryostat (2 W/m) and $P_{tot\ ac}$ is the total electrical power for the RF system assuming a refrigerator efficiency $\eta = 1/400$ at 4.2^oK and we also assume that all but 1% of the higher-order-mode losses are coupled out of the cavity. There are no coupling losses included. Here again as in the case of the SLAC-type linear accelerator

we arrive at unrealistically long accelerators and/or high electrical power demands.

In the remainder of this section we will discuss developments necessary to reduce the lengths and the power consumption of a linear collider system. This we will do for a conventional type or "warm" linac structures since the gradient limitations for superconducting structures seems to be much more fundamental and not accessible to known scaling laws.

The particle energy available from a structure of length L, excited with a klystron pulse power $\hat{P}$, shunt impedance r and attenuation constant τ is given by[15)]

$$E^2 = (1 - e^{-2\tau})\, \hat{P} r \ell \tag{3.5}$$

We assume only traveling wave structures since they require less power for the same gradient as was pointed out in Ref. 16. The value of τ is determined by the mechanical dimensions of the accelerating structure and is related to the filling time t_f (the time needed for a RF pulse to travel through a whole accelerator section) by

$$\tau = \frac{\omega}{2Q}\, t_f \tag{3.6}$$

where $\omega = 2\pi\nu_{RF}$.

From (3.5) and (3.6) we now get

$$\hat{P} t_f = \frac{2\tau}{(1-e^{-2\tau})}\, \frac{E\, g}{\omega\, r/Q} \tag{3.7}$$

where g is the energy gradient ($g = E/\ell$)

The electrical power is given by

$$P_{ac} = \frac{1}{\eta} \hat{P} t_f \cdot \nu_{rep} \tag{3.8}$$

($\eta = 0.3$ is the ac to RF conversion efficiency for SLAC klystrons) and finally we get

$$P_{ac} = \frac{1}{\eta} \frac{2\tau\, Eg}{(1-e^{-2\tau})\omega \frac{r}{Q}} \nu_{rep} \tag{3.9}$$

This equation gives us important clues as to where one should try to improve or change parameters in order to reduce the electrical power to reasonable levels. Since in this section we deal with linac structures we will discuss only the parameters related to the linac. First, we notice that the RF frequency should be chosen as high as possible especially since $r/Q \sim \omega$ and, therefore, $P_{ac} \sim \omega^{-2}$. We also would like to make $\tau \ll 1$. For the structure this means opening up the holes between cavities or, in other words, increasing the group velocity of the RF wave in the linac structure. There is a limit, though, since r/Q depends on τ in such a way that r/Q is reduced as τ is reduced.[15] Detailed studies on accelerating structures will determine the optimum value for the attenuation constant τ.[17] Great effort has to be spent on increasing the ac to RF conversion efficiency for pulsed klystrons beyond the present 30%. For DC klystrons an efficiency of 65 to 70% has been reached.

The choice of the gradient g cannot be made on the basis of Eq. (3.9) alone. There is an optimum between the length of the linear collider $L = E/g$ and the power consumption $P_{ac} \sim E/L \sim g$. Obviously, the optimum collider length cannot be found on a general basis but must be determined

by taking into consideration all the factors involved for a particular site and project. For this and the following section we assume that the collider length should be as short as possible to save real estate and construction costs at the expense of operating costs.

Possible accelerating structures for large linear colliders have been studied and compared[17] and it was found that the so-called "jungle gym" structure (Fig. 4) for example seems to fulfill our requirement for a high energy linear collider. Applying the results of Ref. 17 to our design example we get for three different frequencies the parameters in Table 3.3:

Table 3.3
Linac Structure Parameters[17]

ν_{rf} (MHz)	2856	4040	5712
τ	.20	.35	.57
t_F (μsec)	.20	.20	.20
r/Q (Ω/m)	6670	9470	13000
r (mΩ/m)	60	71	85
g (MeV/m)	100	100	100
$\eta P_{ac}/\nu_{rep}$ (MW sec)	2 x .35	2 x .20	2 x .13
P_{ac} (MW)	2 x 540	2 x 307	2 x 193

It does not seems we have gained much in terms of electrical power compared to a SLAC type linac. Note, however, that now the linac is only 3.5 km long whereas it was 20.6 km in Table 3.1. If we apply to this jungle gym structure the gradient of Table 3.1 (g = 17 MV/m) instead of the assumed value of g = 100 MV/m we would end up with P_{ac} = 2 x 92 MW for ν_{rf} = 2856 MHz. Now we see that we have gained about a factor of five in electrical power compared to a disk loaded wave guide.

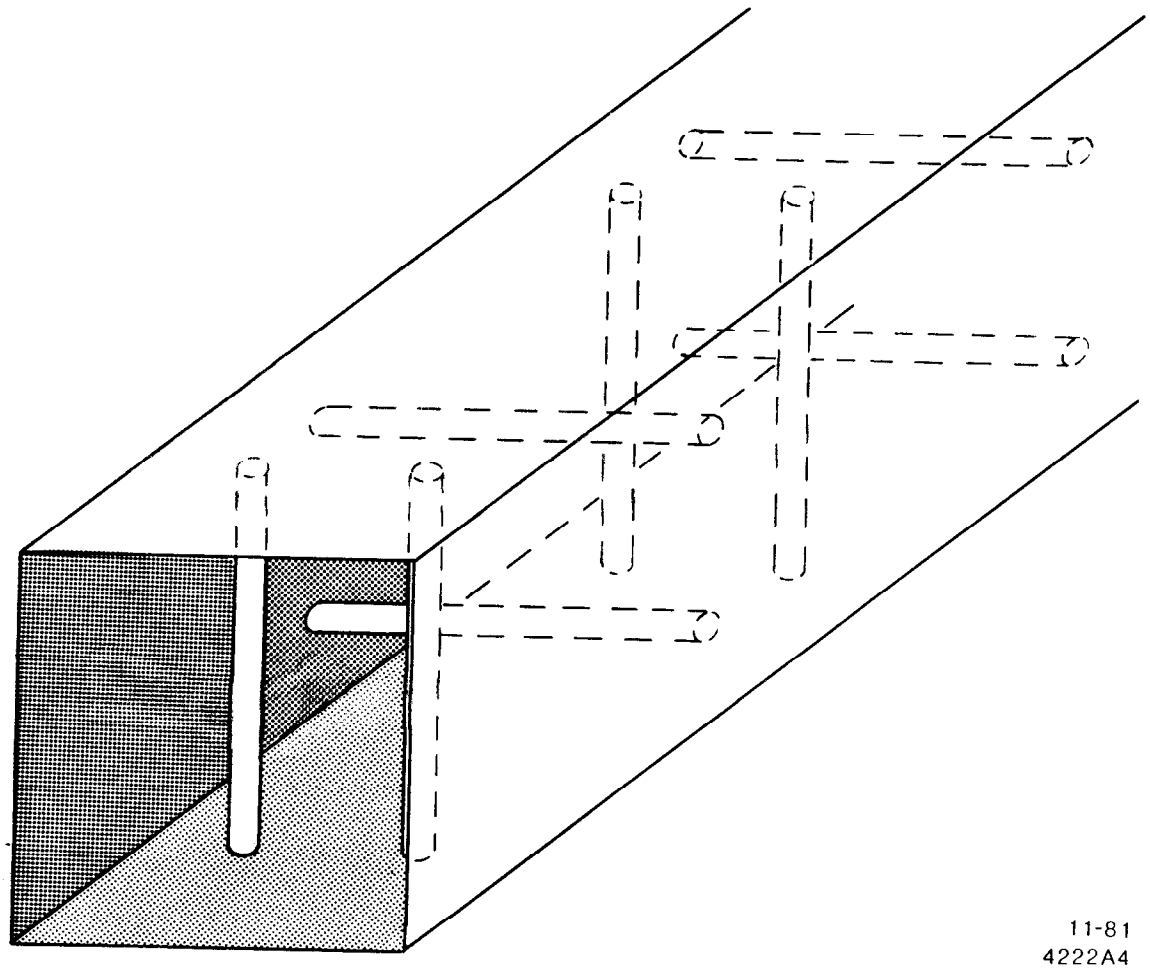

Fig. 4: "Jungle Gym" Accelerating Structure[17)]

This reduction in electrical power, however, is only partly due to the different type of structure. Most of it is due to the reduced filling time of only .2 μsec compared to .8 μsec for the SLAC type structure. This leads us immediately to the next problem. How do we generate rf-pulses of high peak power but short pulse duration.

We are looking for a rf-pulse length of .2 μsec and a peak power given by Eq. (3.5):

$$\hat{P} = \frac{E\,g}{(1 - e^{-2\tau})r}$$

or

$$\hat{P}_{tot} = 1769 \text{ GW} \quad \text{for } \nu_{rf} = 2856 \text{ MHz} \quad g = 100 \text{ MV/m}$$

and

$$\hat{P}_{tot} = 979 \text{ GW} \quad \text{for } \nu_{rf} = 4040 \text{ MHz} \quad g = 100 \text{ MV/m}$$

The rf peak source power then is given by $\hat{P}_{tot}/N_s$ where N_s is the number of sources along the linac. Here again we are unable to find an optimum. If we assume, for example, that the peak power of a rf-source cannot be increased beyond the 38 MW of the SLAC klystron we need 46000 or 26000 klystrons. This is certainly impractical. We, therefore, are forced to develope a device which produces a much higher peak power by a pulse compression technique or just by using a newly to be developed rf-power source. Scaling from the SLAC klystron which can produce 38 MW during a 5 μsec pulse it should be possible to develope, for example, a source for 1 GW peak power during a 200 nsec pulse.

Several ideas are being persued for rf-power sources for extremely high peak power and very short pulse durations.[17)18)] We are not able to predict which of the ideas will result in a feasible technical solution. Since, however, we do not see yet a fundamental obstacle to reach a suitable power source we assume for now that an appropriate research and development program will eventially produce such a rf-source.

4. PARAMETER OPTIMIZATION

The title of this section is somewhat misleading since we will not be able to derive algebraic formulas defining an optimum design. A linear collider facility is still too new a technique and too complicated to have "an optimum set of parameters". What is optimum depends on what aspect one looks at and the real optimum most probably will not be an algebraic one but one which is defined by technical and economic limitations. In this section we will start again with the parameter set of Table 2.1 and we will discuss the consequences of changes of certain paramters.

As a result of the discussions in the previous sections we have for our model linear collider facility a set of parameters as shown in Table 2.1 and Table 3.3. For all frequencies the electrical power consumption is still enormous. To reduce that we have to either (Eq. (3.9)) increase the length of the facility ($g \sim 1/L$), reduce the pulse repetition rate or increase the rf-frequency. The first cure is based on economic reasons and therefore cannot be discussed here further. There is, however, one physical reason not to go to too long linacs. This is the interaction of the beam with the structure through wake fields and the damage done to the beam by these wake fields increases with the length of the linac. Reduction of the pulse repetition rate is an easy cure to reduce power consumption but it also reduces the luminosity. Here we have a direct relationship between the money spent to operate the facility and the physics output.

The rf-frequency has a strong impact on the electrical power consumption since $P_{ac} \sim \omega^{-2}$. In Table 3.3 we see a drop in the power to almost one third going from .3 GHz to 5.7 GHz. There are limitations, however, going to higher frequencies like increased wake fields, problems with power sources and a reduced limit for the maximum bunch length. A research and development program will finally determine the highest feasible frequency.

For our design example we have made an arbitrary choice for σ_ℓ, $\Delta E/E$ and R and we will discuss now the consequences if we change the values of these parameters.

: bunch length σ_ℓ.

The bunch length σ_ℓ should be large to reduce the pulse repetition rate (2.10) and increase the beam spot size (2.7) which is desirable to avoid excessively tight tolerances on the stability of the beam positions at the interaction point. There are however, two independent limits for the bunchlength: the rf-frequency and the number of particles in the bunch (2.9). The higher the rf-frequency the shorter the bunchlength has to be to get uniform acceleration for all particles. For a given accelerator the maximum number of particles in a bunch is limited by wake field effects which increase as the rf-frequency is increased.[19] We, therefore, have to expect a lower beam intensity limit as the rf-frequency is increased.

: energy spread $\frac{\Delta E}{E}$ due to beam strahlung

The allowable energy spread $\Delta E/E$ affects the other parameters in a similar way as the bunch length, however, the maximum value is not determined by any technical consideration but by the desired energy resolution in high energy physics experiment. This limits the energy spread in general to $\Delta E/E \lesssim \pm 2\%$.

: beam aspect ratio R

With increasing aspect ratio the number of particles per bunch increase (2.9) but the pulse repetition rate (2.10) and the beam height decreases. From the power consumption point of view we would like to increase R, however, we reach a limit again where the increased beam intensity causes intolerably strong wake field effect and/or the beam height becomes so small that the required beam position stability cannot be met any more.

We have come to a point where too many parameters are left open due to the lack of having an actual prototype of a linear colliding beam faility. Technical limitations have determined how far we can go with some of the parameters. A good example is the number of particles per bunch. The luminosity could be increased at no extra power cost because the beam only uses a very small percentage of the energy stored in the accelerating structure. Yet, the actual limit is set by wake field effects in the linac and these depend on alignment tolerances and beam control capabilities. It is clear that the limits on these quantities ultimately can be determined only in an actual machine.

To get a feeling, however, how sensitive some parameters influence others some of the main parameters for four different designs of a large colliding beam facility are compiled in Table 4.1. The first set is the design example we have used so far, the second set is a variation of this example. The third set is the result of a ICFA workshop [20] and the last is taken from a design study done in Novosibirsk.[20)21)] In the last example the parameters do not all agree with our scaling laws. This is because in this scheme four beams are brought into collision in such a way as to compensate for the beam beam forces at least to the 1% level. The

Table 4.1

Parameters for Different Colliding Beam Facilities

	Example I	Example II	ICFA	NOVOSIBIRSK
Energy/Beam (GeV)	350	350	350	350
Luminosity no pinch ($m^{-2}sec^{-1}$)	10^{36}	10^{36}	10^{37}	10^{37}
with pinch	$6 \cdot 10^{36}$	$3.5 \cdot 10^{36}$	$3.5 \cdot 10^{37}$	$4.5 \cdot 10^{37}$
Length (km)	2 x 3.5	2 x 3.5	2 x 17.5	4 x 3.5
Beam aspect ratio $R = \sigma_x^*/\sigma_y^*$	7	1	1	3.3*
Bunchlength σ_ℓ (mm)	2	2	3	3
Energy spread $\Delta E/E$ (%)	2	2	1	.1*
Disruption parameter D	4	2	2	2.4*
Beam height σ_y^* (μm)	0.20	0.45	0.59	0.15
Beam width σ_x^* (μm)	1.40	0.45	0.59	0.51
Cross section $(\sigma_x^* \sigma_y^*)^{1/2}$ (μm)	0.53	0.45	0.59	0.28
Beam intensity N	$9.8 \cdot 10^{10}$	$5 \cdot 10^{10}$	$5.7 \cdot 10^{10}$	$100 \cdot 10^{10}$
Pulse rep. rate ν_{rep} (sec^{-1})	460	1023	13646	10*
Beam emittance ($\beta^* = 0.01$ m)				
$\psi_x = \gamma\varepsilon_x$ (m)	$1.3 \cdot 10^{-4}$	$1.4 \cdot 10^{-5}$	$2.4 \cdot 10^{-5}$	$1.8 \cdot 10^{-5}$
$\psi_y = \gamma\varepsilon_y$ (m)	$2.7 \cdot 10^{-6}$	$1.4 \cdot 10^{-5}$	$2.4 \cdot 10^{-5}$	$1.5 \cdot 10^{-6}$
Coupling $K = (\varepsilon_y/\varepsilon_x)^{1/2}$ (%)	14	100	100	29
Damping ring parameter				
$\nu_{rep}/N_B N_s$ (sec^{-1})	230	91	141	10
$N_B N_s$	2	11	97	1*
E_D (GeV)	2.2	1.0	1.4	1.1
ρ_D (m)	3.5	1.8	2.5	2.0
I_D (ma/bunch)	106	106	87	1910
Beam power P_B (MW)	2 x 2.5	2 x 2.9	2 x 43	4 x 0.6
Electrical power† P_{ac} (MW)				
for ν_{rf} = 2856 MHz	2 x 540	2 x 1200	2 x 3180	4 x 12
4040 MHz	2 x 310	2 x 680	2 x 1820	4 x 6.7
5712 MHz	2 x 190	2 x 430	2 x 1150	4 x 4.2

†No energy recovery is assumed yet.

effect of this compensation is included in the parameters of Table 4.1. The quantities that have been modified from the scaling laws due to the compensation scheme are indicated by an asterik (*).

To calculate the damping ring parameter we have to keep in mind that Fig. 2 gives the parameters for full coupling K = 1. If a coupling $K \neq 1$ is desired we proceed as follows. From the scaling law (2.8) we get the desired beam emittances ψ_x, ψ_y. These we reduce to one emittance ψ_D from $\psi_x = \psi_D 2/(1 + K^2)$, and $\psi_y = \psi_D 2K^2/(1 + K^2)$ by eliminating the coupling K and use ψ_D in Fig. 2 to get the other parameters.

In Table 4.1 we find vastly different requirement for the electrical power demand. High power levels are either the result of a poor choice of parameters or due to a high luminosity. In order to fairly compare the different designs the electrical power demand has to be based for the same luminosity ($\mathscr{L} = 1 \cdot 10^{36} m^{-2} sec^{-1}$) for all design examples. We have also included the luminosity enhancement due to the pinch effect. For this case we get the parameters of Table 4.2.

Table 4.2
Power Demand Based on Equal Luminosity

Power for same Luminosity	Example I	Example II	IFCA	Novosibirsk
$\mathscr{L}$(with pinch)($m^{-2} sec^{-1}$)	10^{36}	10^{36}	10^{36}	10^{36}
Particles Beam (1 Bunch)	$9.8 \cdot 10^{10}$	$5 \cdot 10^{10}$	$5.7 \cdot 10^{10}$	$100 \cdot 10^{10}$
ν_{rep} (sec^{-1})	77	290	390	0.22
Beam power P_B (MW)	2 x 0.42	2 x 0.83	2 x 1.23	4 x 0.013
Length of Collider (km)	2 x 3.5	2 x 3.5	2 x 17.5	4 x 3.5
Electrical power P_{ac} (MW) for ν_{rf} = 2856 MHz	2 x 90	2 x 340	2 x 91	4 x 0.26
4040 MHz	2 x 50	2 x 194	2 x 50	4 x 0.15
5712 MHz	2 x 32	2 x 123	2 x 32	4 x 0.09

Here we see that Example II is still at a very high power level and Example I shows that a significant reduction can be achieved choosing different input parameters. The modified ICFA example turns out to be equivalent in power and luminosity to Example I, however, note that the length of the facility is 5 times longer which due to (Eq. 3.9) has reduced the power by a factor five. A heavy price is thereby paid for the choice of a smaller energyspread due to beam strahlung of 1% instead of 2% in Examples I and II. The actual total energyspread in the beam, however, might not be smaller anyway because of the long bunchlength of σ_ℓ = 3 mm. It will be very difficult to obtain uniform acceleration within that long a bunch in the presence of wake fields in a S-band linear accelerator.

The Novosibirsk design with space charge compensation is the most appealing from the power consumption point of view. However, this design implies parameters which are very difficult to achieve. The beam intensity is a factor of 10 to 20 higher than in the other examples. From what we know theoretically and experimentally at SLAC we think this not yet feasible. New ideas for structure design and/or beam control have to be developed to accelerate that intense a bunch. In addition the compensating scheme to 1% requires very accurate beam control. The four linac pulses have to be timed to better than 0.1 psec and the intensities of the four bunches are to be kept equal to 1%. Although this design is pushing parameters beyond the present state of the art the returns (low operating cost at high luminosity) are dramatic and worth intensive study and development.

We have not been able to really develope an optimized design but we have arrived at a set of parameters in Example I which gives a luminosity in excess of $10^{36} m^{-2} sec^{-1}$ at a center of mass energy of E_c = 700 GeV with parameters which seem to be technically feasible and at a power consumption

which is equal or less (depending on the rf-frequency) than that of the storage ring LEP at a center of mass energy of only $\sim$ 170 GeV.[2)]

To maximize the physics output for a facility it is very important that more than one experiment can be operated at the same time. In a linear collider facility this is possible. Since only a very small fraction of the energy stored in the accelerating structure is taken out by the beam we can accelerate more than one bunch at no additional power cost. The energy of successive bunches would be different, however, depending on the rf-energy left in the structure at the moment a particular bunch is accelerated. At the end of the linacs a dc magnet system splits the bunches apart according to their energy and directs them to various experiments. Other schemes for more than one experiment have been proposed[20)] but in these schemes the interaction points are all along the linac axis and only one experiment at a time would receive luminosity. A multiple bunch scheme to serve more than one experiment at a time is not possible in these schemes because of the beam beam disruption. After a bunch has collided with another bunch the pinch effect makes that bunch unusable for further collisions. In addition the bunches would have to be separated longitudinally by more than .1 to .2 μsec since the distance between interaction points cannot be made smaller due to the space required for the focusing system and the size of the detectors. If successive bunches are separated by .1 to .2 μsec we need to lengthen the rf-pulse beyond the filling time of the structure and thus we have lost all advantage of multiple bunch acceleration. We may as well pulse the linacs more often and share pulses to more than one experiment.

5. PARTICLE PRODUCTION AND POLARIZATION

For a linear colliding beam facility we have to consider the production of very intense pulses of electrons and positrons.

In addition the physics potential at the very high center of mass energies of colliding linac beams is greatly enhanced if we are able to produce polarized beams. We will see in this section that polarized electron as well as positron beams can be produced.

5.1 Electron Production

Non polarized electrons can be produced in many ways. Here at SLAC we produce them either with a thermionic gun[15.)] or by photo emission from a Ga As surface.[22)25)]

In a thermionic gun electrons are emitted from an indirectly heated barium or strontium oxide surface. Such a gun has been built[23)] for the SLAC Linear Collider Project and has produced more than 10^{11} electrons[24)] in a pulse short enough to be compressed into a S-band bunch by a special buncher section.

The second type of gun used at SLAC is a photo emission gun. Here a strong laser pulse is used to release electrons from a gallium arsenide (Ga As) surface.[22)] The advantage of this gun above a thermionic gun is that by using a circularly polarized laser pulse on a Ga As cathode that is cooled down to liquid nitrogen ($77^{o}K$) longitudinally polarized electrons can be produced.[25)] Here again the intensity does not seem to be a problem with the lasers available although a definitive test will be made at SLAC only by the end of this year.

5.2 Positron Production

Non-polarized positrons can be produced by striking a high Z target with high energy electrons. The electrons generate high energy photons by bremstrahlung which then disintegrate into electron and positron pairs. The positrons emanating from the target material are collected by a focusing system and accelerated in a subsequent linac.[15)26)]

The required number of positrons in the order of 5 to 10 x 10^{10} demand an improvement of present day converters by about an order of magnitude.[7)] We cannot increase the electron beam intensity above the positron beam intensity since we have assumed that the beam intensity is limited by wake field effects, each electron has to produce at least one useful positron. The intensity can be calculated from.[26)]

$$\frac{N^+}{N^-} = 0.24\ E^-(\mathrm{GeV}) \int_0^{\Delta E^+} \Omega^+(E^+)\ dE^+ \qquad (5.1)$$

where E^- is the electron energy at the target, ΔE^+(MeV) the range of positron energies and Ω^+(sr) the solid angle that can be focussed into a subsequent linace aperture.

If the electron energy E^- and the acceptance of the focusing system (Ω^+) is sufficiently large we can reach a one to one convertion from electrons to positrons.[7)] A totally different way of creating positrons was proposed using a wiggler magnet.[27)28)] In this scheme one of the linear collider beams would after it had collided with the other beam be guided through a wiggler magnet. Through synchrotron radiation high energy

gamma rays are produced which in turn are aimed at a thin target to produce electron positron pairs. The advantages are that the thermal heat load on the target is greatly reduced since the electron beam does not strike the target any more and second by using a helical wiggler the gamma rays are circularly polarized and can create longitudinally polarized positrons.[27] For simplicity we treat hear only the flat wiggler to demonstrate the principle. The properties of a helical wiggler are discussed in more detail in Ref. 29.

The number and energy of photons produced per electron depends strongly on the wiggler parameters and the electron energy. The wavelength of the photons for a parallel beam in the forward direction is given by

$$\lambda_o = (\lambda_w/2\gamma^2) \cdot (1 + \frac{1}{2} K^2) \tag{5.2}$$

where $K = \lambda_w \, ecB_w/2\pi \, mc^2$, λ_w the length of the wiggler period and B_w the wiggler field. If $K > 1$ the transverse motion of the particles in the wiggler is relativistic which modifies the otherwise pure sinusoidal motion. As a consequence higher harmonics of the fundamental wavelength λ_o appear.[30] We will ignore these complications and assume wiggler parameters which give a value $K = 1$. In this case if we observe the photons on axis we can expect a single spectral line given by Eq. (5.2). The energy of the photons is given by ($K = 1$):

$$E_\gamma = \frac{4}{3} \gamma^2 \, \hbar c \, \frac{2\pi}{\lambda_w} \tag{5.3}$$

The total radiated energy of an electron is just[5] $P_\gamma \cdot \Delta t \cdot 2N = P_\gamma \cdot (\lambda_w/2c) \cdot 2N$ or

$$\Delta E = \frac{8}{3} \pi^2 \, r_e \, mc^2 \, \gamma^2 N \, \frac{K^2}{\lambda_w} \tag{5.4}$$

where 2N is the number of wiggler poles. From Eqs. (5.3) and (5.4) we get for the number of photons

$$\mathcal{N}_\gamma = \frac{4}{3}\pi \frac{r_e mc^2}{\hbar c} K^2 N = \frac{4}{3}\pi \alpha K^2 N \qquad (5.5)$$

with $\alpha = e^2/\hbar c = 1/137$.

We see from this equation that the number of the photons produced in the wiggler depends only on the number of the magnet poles and is independent of the electron energy.

The photons from the wiggler magnet are aimed at a high Z-material target to produce electron positron pairs. The positron yield per electron is given by [32]

$$N^+/N^- = \mathcal{N}_\gamma(\sigma_p N \cdot X_t) \cdot \frac{t}{X_t} \frac{\Delta E^+}{2E^+} \qquad (5.6)$$

where $N = N_{MOL}\, \rho_t/A_t$; $N_{MOL} = 6 \cdot 10^{23}$, ρ_t is the specific weight and A_t the atomic number of the target material, σ_p the pair production cross section, X_t the radiation length, t the target thickness and $\Delta E^+/E^+$ the relative energy acceptance of the positron focusing system.

For a tungsten target the photon energy E_γ and the quantity $\sigma_p N X_t$ is plotted in Fig. 5.

For the wiggler magnet we assume a field of B_w = 10 kG, a period length of λ_w = 1 cm and a total length of L_{tot} = 100 m. The number of magnet poles then is 2N = 20000. From this wiggler each electron will radiate $\mathcal{N}_\gamma$ = 306 photons with an energy of $E_\gamma(\text{MeV}) = 4.7 \cdot 10^{-4}\, E^2(\text{GeV}^2)$. In Fig. 6 we show the positron yield we may expect from this system assuming that we can accept a total positron energy spread of $\Delta E^+/E^+ = 50\%$. The target thickness assumed is $t/X_t = 0.1$ independent of the photon energy.

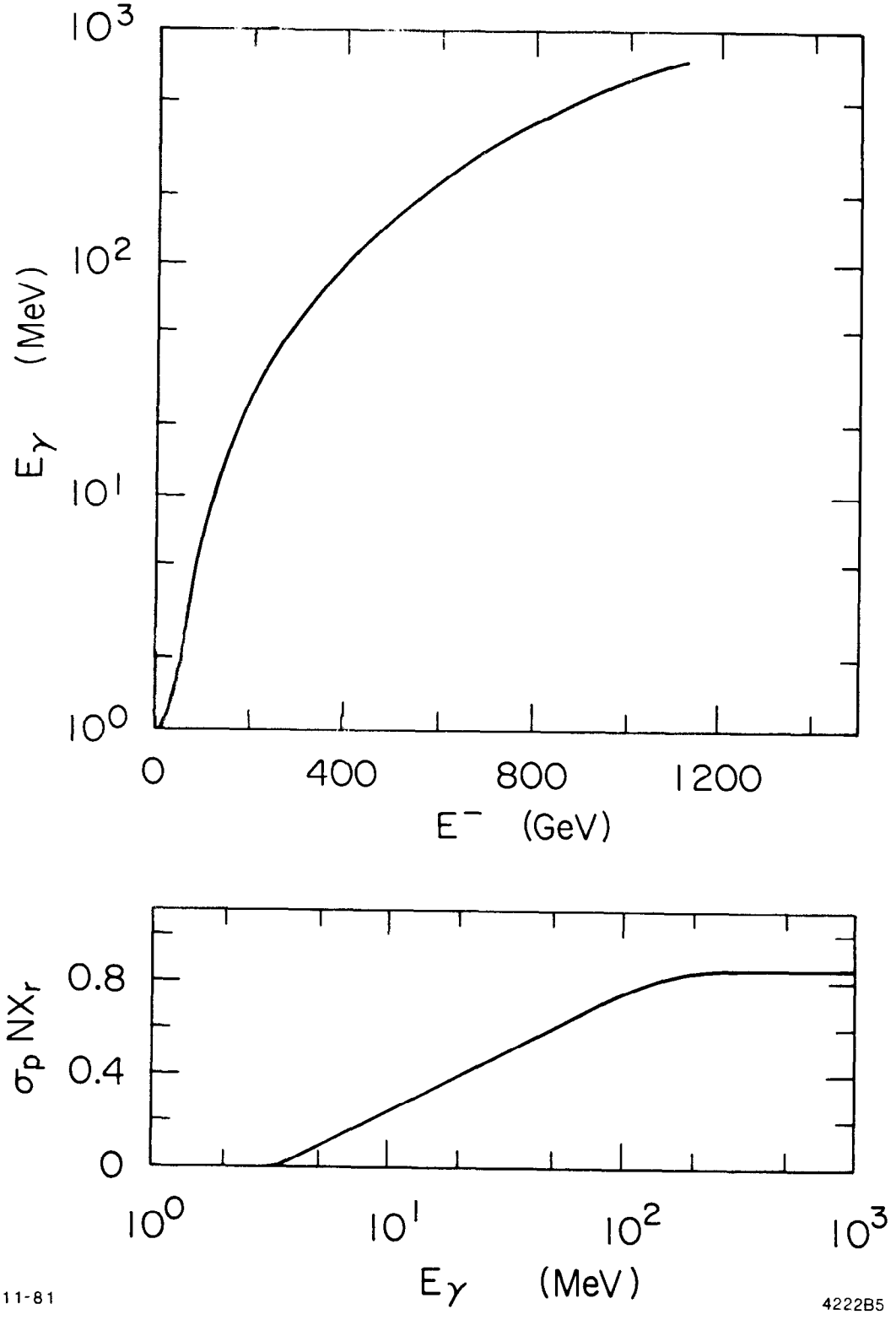

Fig. 5: Photon Energy and Pair Production Cross Section

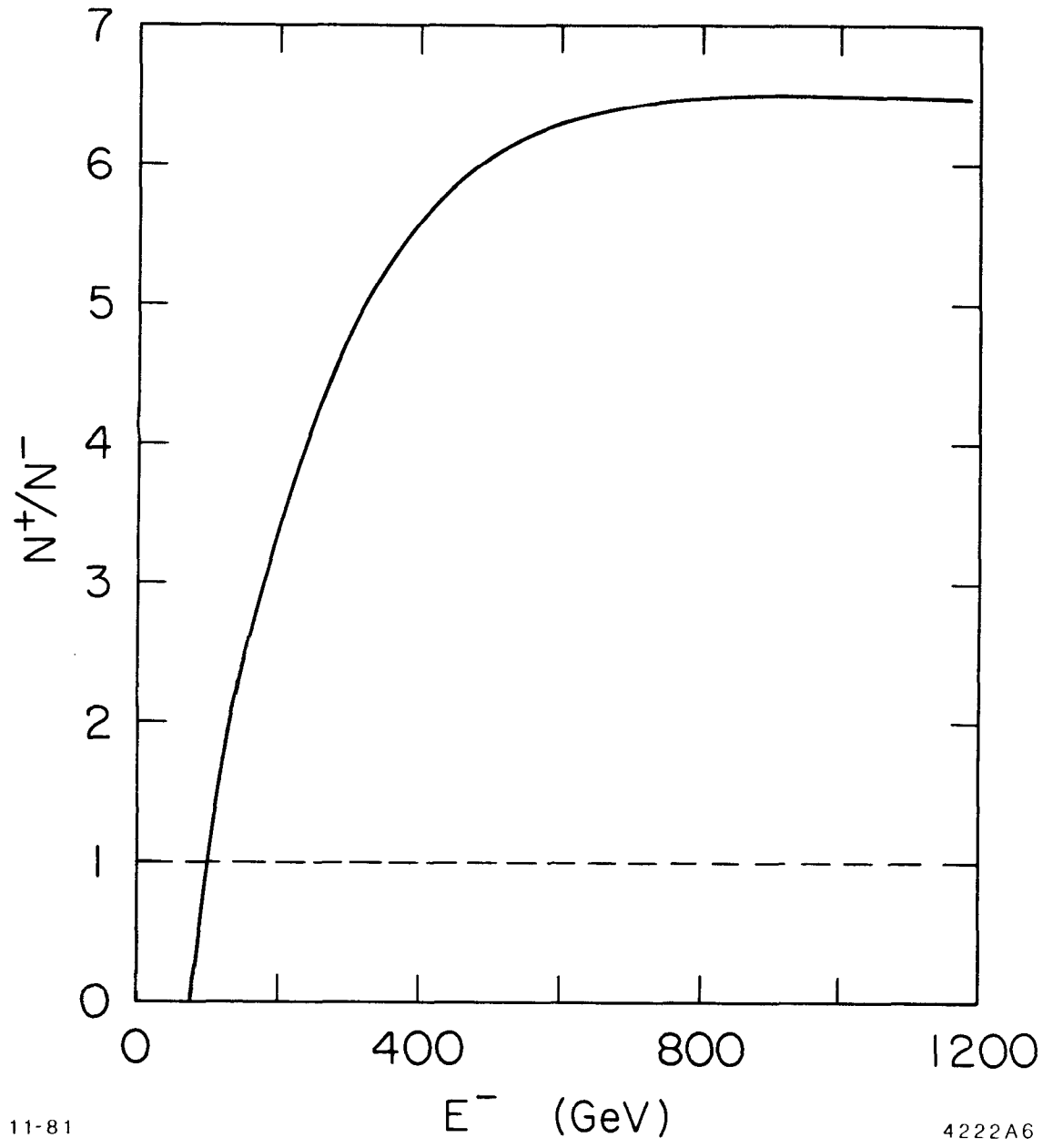

Fig. 6: Positron Production Efficiency

This somewhat arbitrary choice was made to simplify the calculation rather than to optimize it. In a real design the target thickness has to be determined from a compromise between positron yield and multiple scattering which depends on the positron energy. For higher beam energies the chosen target thickness, however, is close to the optimum choice. From Fig. 6 we immediately see that the electron energy has to be of the order of 150 GeV or higher in order to produce more than one positron per electron.

To produce longitudinally polarized positrons we use a helical wiggler. Strong and short period helical wigglers can be built from permanent magnets.[33] The flux of circularly polarized photons in general is comparable to that of a flat wiggler and so is the photon energy. We will not be able to go into more detail here but have to refer to references 27, 29 and 34. In Ref. 27 the result of a more detailed calculation for a particular case shows that half of all produced positrons have an average polarization of about 70%. Since the positrons with poor polarization all have a low energy and therefore easily can be separated out we can expect a positron beam with 70% polarization if every electron now produces at least two positrons on the target. From Fig. 6 we see that this is possible at sufficiently high energies.

In a linear collider its a long way from the source of particles till they collide and much care has to be exercised to preserve the polarization. This it specially true for longitudinally polarized beam. All particles have to pass through a damping ring and it is well known that the polarization of a beam has to be aligned with the direction of the magnetic field of the bending magnet which normally is in the vertical plane. Precession of a longitudinally polarized beam in a vertical bending field would smear out the polarization due to the finite energyspread in the beam. A scheme has been proposed to both preserve the polarization

in the damping ring and after ejection to rotate the spin in any direction desired.[35] For this we need a specific design of the beam transport system to the damping ring and from the damping ring to the linear accelerator. Rotation of the spin direction is accomplished by both a transverse and a longitudinal magnetic field. In a transverse field the rotation of the spin component normal to the field is given by

$$\psi_{\perp} = \frac{e}{m} \eta \left(1 + \frac{1}{\gamma}\right) B_{\perp} \ell \qquad (5.7)$$

where $\eta = (g-2)/2 = 0.00115965$, g the gyromagnetic constant and $B_{\perp} \ell$ the intergrated transverse magnetic field strength. Apart from a small term $1/\gamma$ the spin rotation is independent of the energy. In other words the spin of a particle can be rotated by 90° in a magnetic field of 23 kG m. A transverse spin can be rotated about a longitudinal axis in a solenoid field where we have

$$\psi_{\parallel} = \frac{e}{E} \left[1 + \eta \frac{\gamma}{1+\gamma}\right] B_{\parallel} \ell \approx \frac{e}{E} B_{\parallel} \ell \qquad (5.8)$$

Here the spin rotation is energy dependent and the necessary rotations should be done at low energies. This becomes obvious from the parameter for the SLC project were we have an energy of only 1.21 GeV at the damping ring. To rotate the spin by $\psi_{\parallel} = \pi/2$ we need a solenoid field of as much as $B_{\parallel} \ell = 63$ kG m.

The process of the spin handling going through a damping ring is as follows. In Fig. 7 we assume a longitudinally polarized beam coming out of the linear accelerator. Through a combination of a transverse field and a solenoid field we generate a vertical spin orientation in the beam. This orientation is in line with all magnets in the damping ring and the

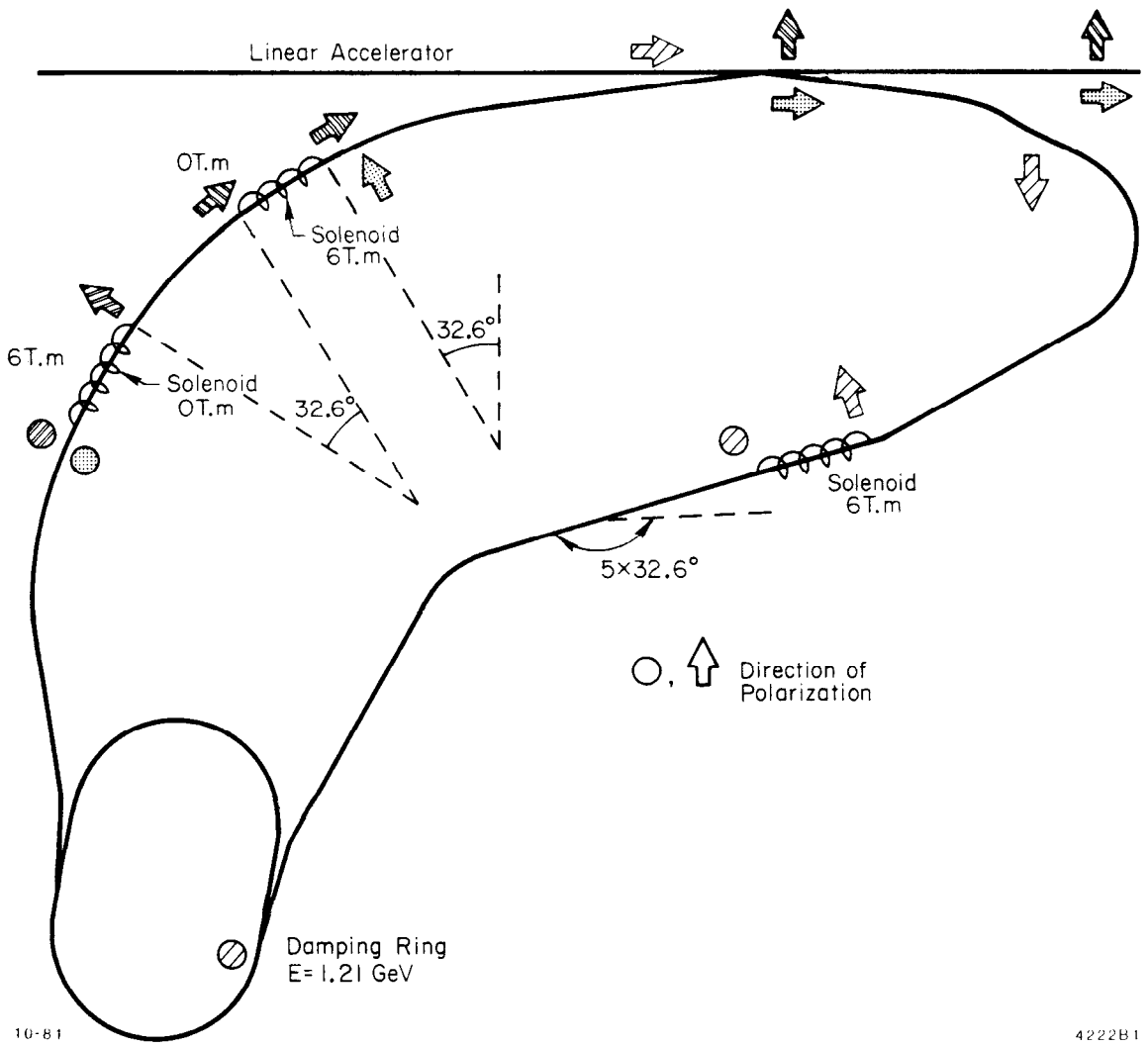

Fig. 7: Polarization Rotators

polarization can be preserved. Coming out of the damping ring the beam passes through a combination of two solenoids and two transverse field sections. Depending on which solenoid is turned on we end up with a longitudinal or transverse polarization at the entrance of the linac. By the use of both solenoids any polarization direction can be realized.

Here we recognize a great simplication in producing arbitrary polarization at the collision point compared to the very elaborate spin rotating systems necessary at either side of each interaction region in a storage ring. In conclusion we find that in very high energy linear colliding beam facilities we find possibilities to produce both polarized electrons and positrons. The direction of the polarization can be chosen freely by adjusting the polarization rotators at the damping rings.

6. INTERACTION OF A BEAM WITH THE ACCELERATING CAVITIES

As a charged particle passes through an accelerating cavities it excites an electromagnetic field in the cavity which will not disappear the moment the generating charge leaves the cavity. The field left in the cavity is called the wake field and it will act back on any particle that passes the same cavity later. The wake fields induced are rather complicated fields depending on the particle distribution in the bunch, the form and dimension of the cavity and the transverse position of the beam with respect to the symmetry axis of the cavity. However, whatever the form of the electromagnetic field, it is known [36] that it can be expanded in normal modes satisfying appropriate boundary conditions of the cavity.

We solve the wave equation

$$\Delta \vec{A} + k^2 \vec{A} = 0 \qquad (6.1)$$

with $\vec{n} \times \vec{A} = 0$ on the metallic boundary ($\vec{n}$ unit vector normal to the surface), $k^2 = \omega^2/c^2$ and ω the mode frequency. The solutions are orthogonal functions $\vec{A}_\alpha$ which we normalize like

$$\int \vec{A}_\alpha(r)\ \vec{A}^*_\beta(r)\ dV = \begin{cases} 0 & \text{if } \alpha \neq \beta \\ V & \text{if } \alpha = \beta \end{cases} \tag{6.2}$$

Any field now can be expanded in mode components:

$$\vec{A}(r,t) = \sum_\alpha a_\alpha(t)\ \vec{A}_\alpha(r) \tag{6.3}$$

Following Condon[37] we also expand the beam current in a similar way:

$$\vec{i}\ (r,t) = \sum_\alpha I_\alpha(t)\ \vec{A}_\alpha(r) \tag{6.4}$$

where

$$I_\alpha(t) = \frac{1}{V} \int \vec{i}(r,t)\ \vec{A}_\alpha(r)\ dV \tag{6.5}$$

If we use Maxwells equation $\text{curl}\vec{H} - \frac{1}{c}\frac{d}{d}\vec{E} = 4\pi\ \vec{i}$ and use (6.3) to (6.5) we get

$$\frac{d^2}{dt^2}\ a_\alpha + \omega_\alpha^2 a_\alpha = 4\pi\ c^2\ I_\alpha(t) \tag{6.6}$$

After solving (6.6) the problem is completely solved for any current $\vec{i}(r,t)$. The actual difficulty in solving the field equations lays in the boundary problem (6.1). Cavity boundaries in general are not expressable in an algebraic equation. Computer programs have been developed therefore to calculate the modes and from them the electromagnetic fields which we call the wake fields.

For simple cases it is possible to calculate the modes analytically. In a particular simple case - two parallel plates-the fields due to a point charge give rise to simple δ-function fields which develope like

shown in Fig. 8.[38] In this case we see how the fields - actual two wave patterns - are bouncing back and forth between the reflecting plates long after the charge is gone. Any charge traversing this "cavity" after the first charge will be affected by these fields. For a real beam with a gaussian distribution for example, the fields are gaussian too but still have the general features of Fig. 8. The situation here is simple because there are no reflections from cylindrical surfaces. In a real cavity we have those reflections which eventually come back to the beam area. The field pattern also will be affected by openings in the cavity walls for the beam to go through.

So far we have considered only cavity structures symmetric about the beam and all the fields on the axis produce only longitudinal components for symmetry reasons. If we now have a cavity with finite openings for the beam and the beam passes through this cavity at a transverse displacement δr from the cavity axis it is not difficult to imagine that modes with transverse fields components (TE modes) are excited.

For a disc loaded linac structure like that of the Stanford Linear Accelerator modes up to very high order have been calculated and summed up to give the total wake field.[19] The longitudinal field and the transverse wake fields are shown in Fig. 9 and Fig. 10. The wakefields are given in volts per pC of charge in the beam for each of SLAC's 86000 cavities. The longitudinal wake fields cause the particles in the tail of a bunch to be decelerated due to the fields created by the head. This energy loss has been measured at SLAC[39] to be 50 MeV for a bunch of 10^9 electrons and agrees with the numerical calculations.

This energy loss which depends on the position of a particle in a bunch is very significant for a linear collider because of the high charge in the

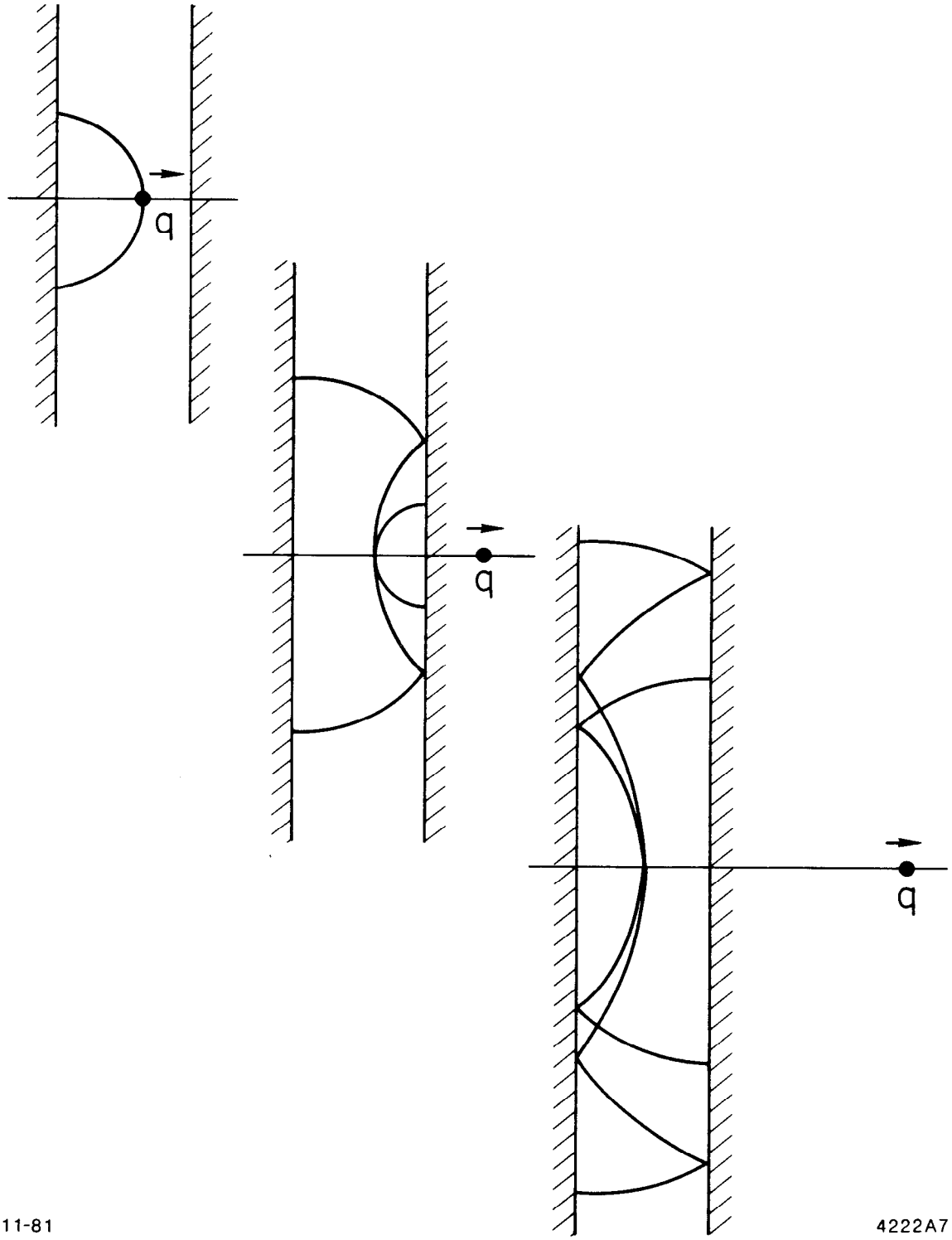

Fig. 8: Wake Fields for a Parallel Plate "Cavity"[38)]

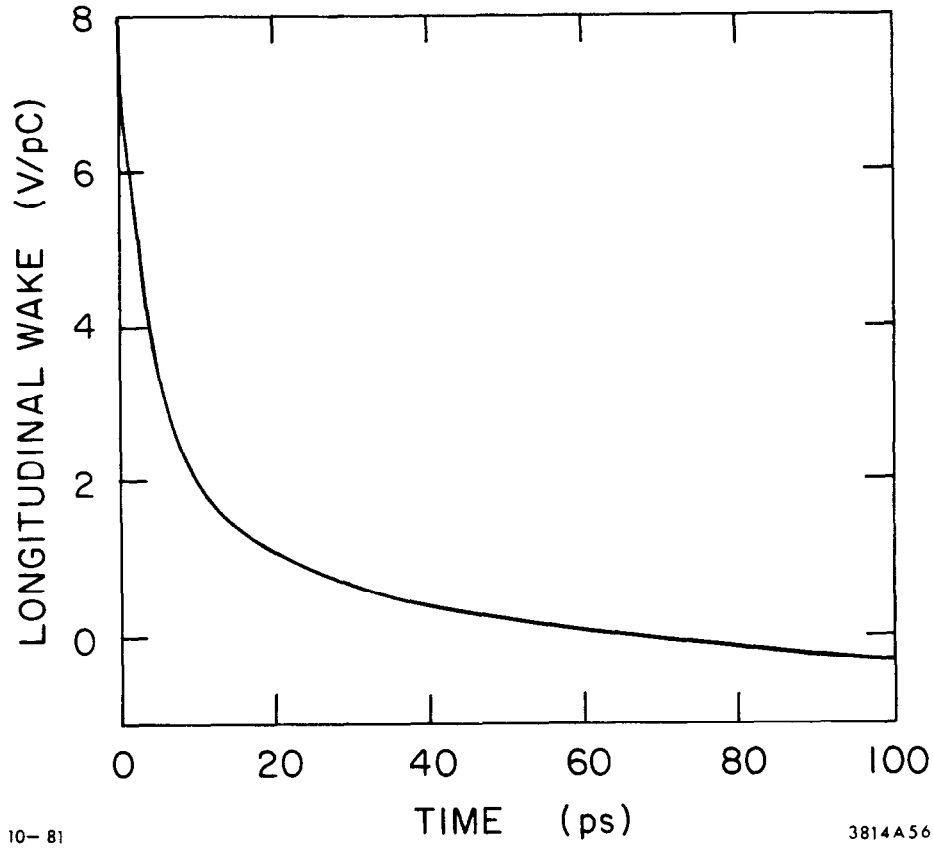

Fig. 9: Longitudinal Wake Field per Cell for the SLAC Structure[7)]

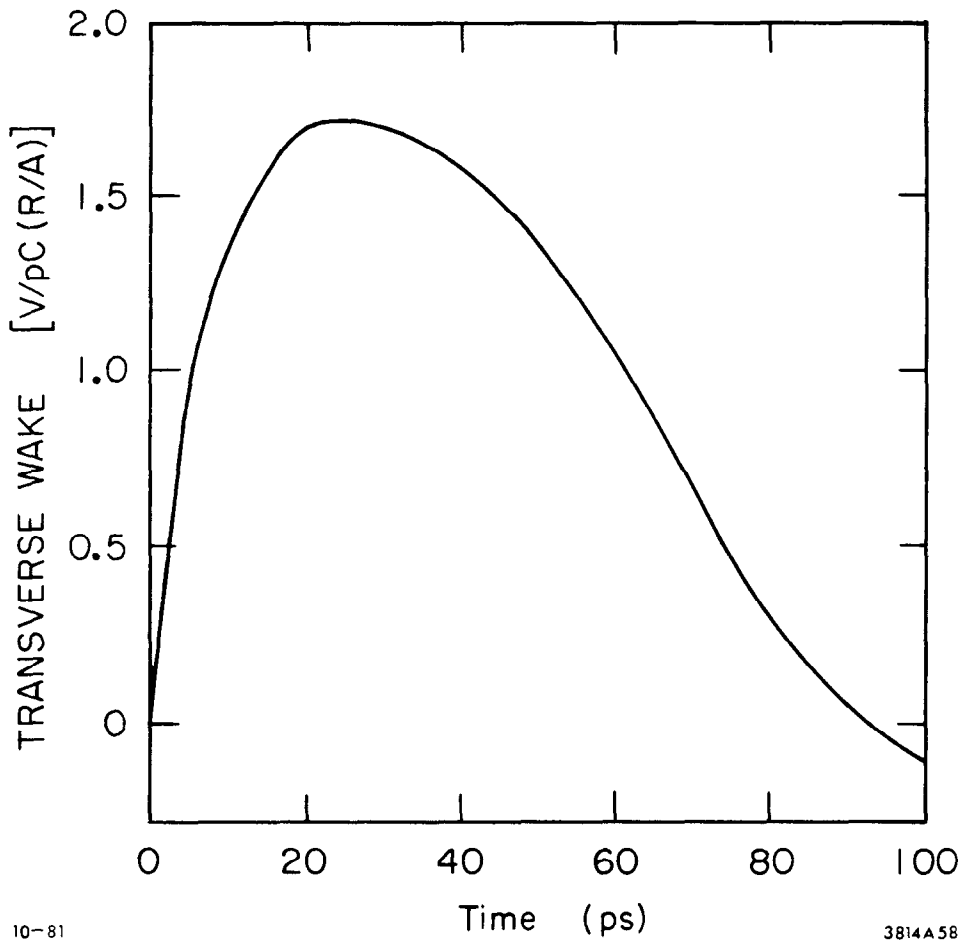

Fig. 10: Transverse Wake Field per Cell for the SLAC Structure[7)]

bunch. By properly shaping the time dependence of the accelerating field the effect of the wake field on the energy spread can be minimized. To do this the bunch is injected at a phase where the accelerating field increases with time such that the particles in the head of the bunch are accelerated less than the particles in the tail. The stronger acceleration for the particles in the tail then is compensated by the decelerating effect of the wake fields.[7] The transverse wake fields can have a serious effect on the beam cross section. To understand the physics we assume a macro particle with charge q to be accelerated in the linac. Due to the focusing force of quadrupoles distributed along the linac this particle executes betatron oscillations according to

$$x_1 = a \cos \omega_\beta t \tag{6.7}$$

where ω_β is the betatron frequency. The transverse force created by this macro particle is given by

$$F_\perp = q \cdot W(\tau)\, x_1 = q\, W(\tau)\, a \cos \omega_\beta t \tag{6.8}$$

where $W(\tau)$ is the transverse wake field at a distance $\Delta s = c.\tau$ behind the charge q.

A test particle behind the macro particle q which also executes betatron oscillations is driven by this wake field and we have for the equation of motions

$$\ddot{x}_2 + \omega_\beta^2\, x_2 = \frac{F_\perp}{m\gamma} = q\, \frac{W(\tau)a}{m\gamma} \cos \omega_\beta t \tag{6.9}$$

We do not have to solve this equation to see that the wake fields drive the test particle at resonance. In a real bunch this resonance leads to increased transverse ocillations of the tail as the bunch passes along the

linear accelerator. In extreme cases the oscillation amplitudes in the tail get as large as the aperture and particles in the tail of the bunch are scraped off, a phenomenon that is called "beam break up".[40)]

In a linear collider system we will notice a damaging effect much earlier. Even a small increase of transverse oscillations of the particles in the tail of the bunch will increase the apparent beam emittance and therefore reduce the luminosity. The cure is simple: do not excite transverse wake fields by steering the beam through the middle of the accelerating structure. It is clear that the alignment of the linac and the ability to carefully steer the beam through the middle of the structure is of utmost importance for the success of a linear collider facility. The tolerances ultimately will limit the maximum number of particles in a bunch. More details of the transverse wake field effect due to missteering of the beam or misalignment of the accelerating structures can be found in Ref. 41.

Present day technology in alignment and beam control in a disk loaded S-band linear accelerator seems to put a limit on the particle number per bunch in the order of 5 to 10 x 10^{10} particles. This is certainly a soft limit but should be of the right order of magnitude. Measurements to be performed at SLAC at the end of this year and next year should illuminate the validity of this limit.

Obviously the excitation of wake fields in newly to be developed structures will have to be kept to a minimum.

From Figs. 9 and 10 we see that the wake fields - longitudinal as well as transverses - decay rather rapidly. This is important for the acceleration of more than one bunch. If we can accelerate several bunches in short distances we are able to deplete the energy stored in the accelerating cavities and serve several experiments without additional power cost. To do this, however, the total length of the bunch train should be less than

the 200 nsec filling time we have assumed for the accelerating structures.

7. FINAL FOCUS SYSTEM AND THE BEAM-BEAM INTERACTION

7.1 Final Focus System

Even so we have taken great care to minimize the beam emittance in the damping ring and during acceleration the beam spot size at the collision point is not small enough yet for a useful luminosity. A special focusing system is required to further reduce the beam size to micron or submicron values. Typically this amounts to a beam size reduction between the end of the linac and the collision point by a factor 50 to 100.

Like in a light optical system we have to expect significant imaging errors due to chromatic aberrations associated with that big a demagnification. To compensate for these chromatic aberrations sextupole magnets are used. The principle of chromatic corrections is as follows:

Particles of the beam which do not have the right energy are focussed different from particles with the ideal energy. Lower energy particles have a shorter and higher energy particles a longer focal length (Fig. 11a). To compensate these chromatic effects we have to separate in space the particles with different energies. This is done by introducing a dispersion function.[9] We therefore need in the final focus system a set of bending magnets which deflect the particles differently so that at some point downstream of the first bending magnet the particles are well separated according to their energies (Fig. 11b). This separation is expressed by the so-called dispersion function of the magnet lattice. At those places, where the dispersion is large we place sextupole magnets. Their property is to be a quadrupole with changing strengths as one moves across the aperture

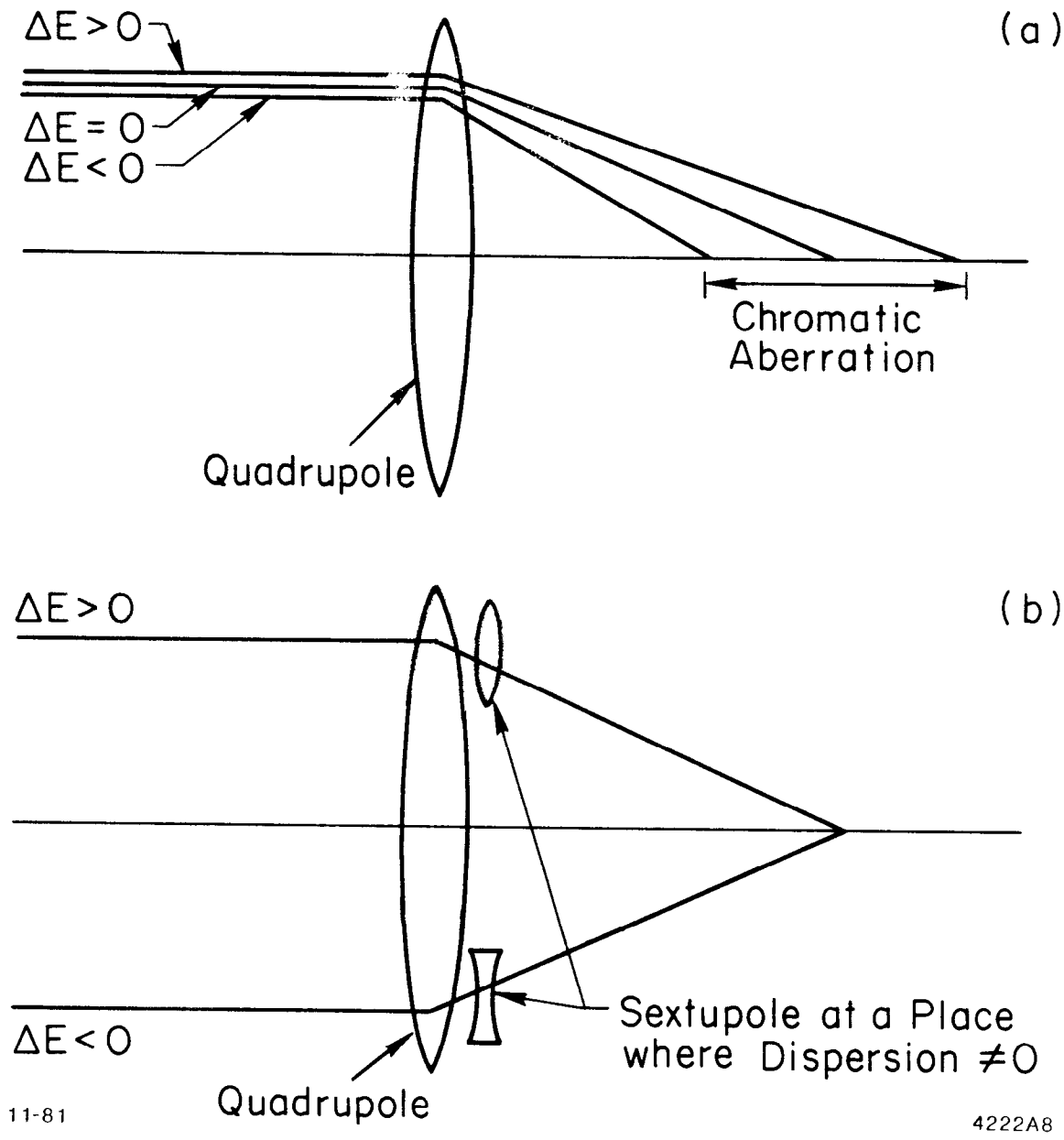

Fig. 11: Principle of the Correction of Chromatic Errors

in the mid plane of the magnet. Especially a sextupole is a focusing quadrupole on one side of the center and a defocusing quadrupole on the other side. This is the arrangement we need for chromatic correction. The higher energy particles, which have not experienced enough focusing in the quadrupoles are, due to the dispersion, all concentrated on one side of the center line. This is the side where we want the sextupole to be focusing to make up for the insufficient quadrupole focusing. A similar argument applies for the lower energy particles Fig. 11b.

This compensation scheme, however, is not free of flaws. Due to the intrinsic nonlinearity of the sextupole field and the finite extend of any monoenergetic part of the beam geometric aberrations are introduced which enlarge the beam spot at the collision point (Fig. 12).

To minimize this effect we have to use at least two sextupoles for chromatic correction. These two sextupoles have to be separated by a half betatron wavelength and they have to be equal in strength. This way the geometric error caused by the first sextupole is compensated by the second sextupole.[42)]

A final focus system based on these correction principles has been designed [43)] for the SLAC Linear Collider and tests with a ray tracing program through the actual magnetic fields have confirmed the validity of the correction principles. Fig. 13 shows the final spot size with σ = 2.1μm where it ideally is supposed to be σ_o = 1.7 μm in radius.[43)] This correspond for the SLC system to an actual demagnification by a factor 58 instead of an ideal 72. Obviously the chromatic correction scheme is suitable for a final focus system in a linear colliding beam facility

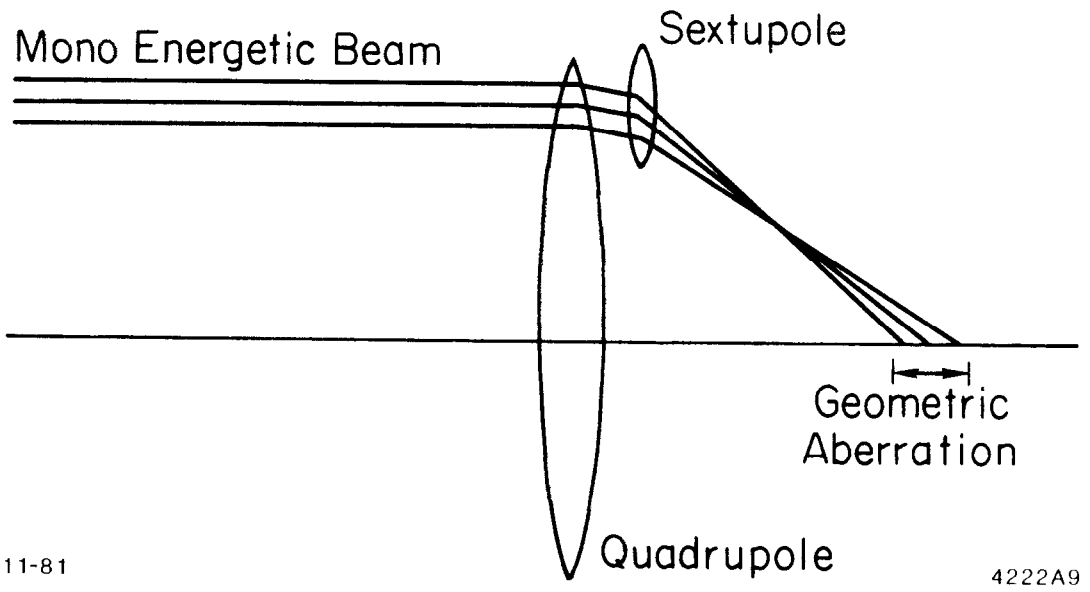

Fig. 12: Cause of Geometric Aberrations

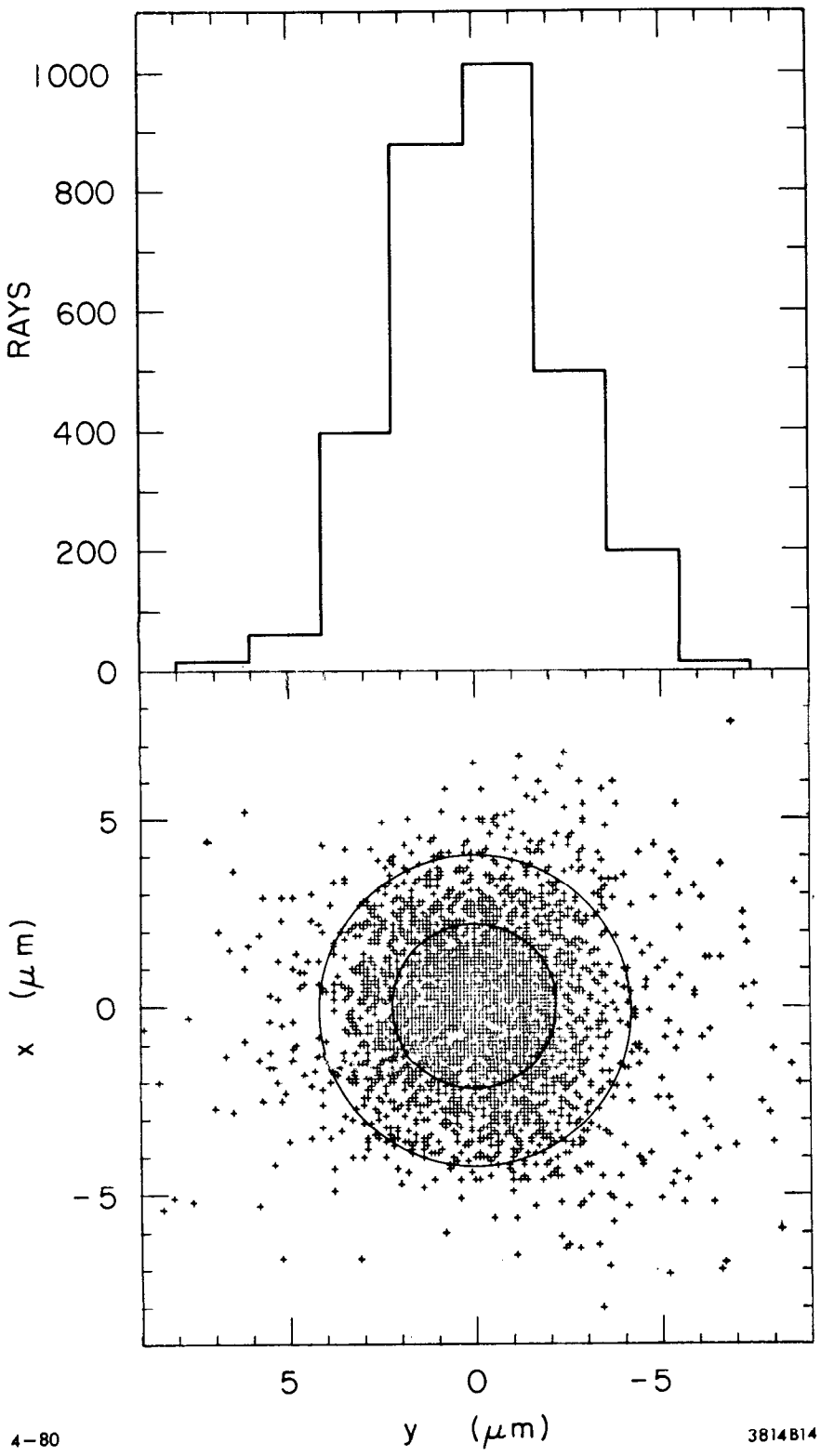

Fig. 13: Beam Spot Size at the Collision Point (Result of Particle Tracking)[45)]

7.2 Beam Beam Effect

Once the beams are focussed down to micron size we are faced with two problems. One is the problem of finding the other beam, the other problem we have to investigate is what happens when the two bunches collide. Will the electromagnetic forces be so strong that the beams destroy each other before we get any significant luminosity.[2)]

It is clear that random fast variations of the beam position from pulse to pulse cannot be tolerated. If we have a beam spot size of ± 1 μm at the collision point a typical beam size in the linac would be about ± 0.1 mm, which is equal to the short term stability requirement for the beam of a linear collider. Slow variations are less severe because they can be detected and corrected for by a feedback system. Suppose, however, the beam position to be absolutely stable in time. We still have to solve the problem of finding the other beam which might be only 1 micron or less in diameter.

Here we get help from the tremendous electromagnetic fields of the beams which act on each other even so they are separated by many beam diameters.

For a beam with 10^{11} particles in a bunch which is only 4 mm long we have a peak beam current of 1200 amperes. This current produces at the surfaces of a beam with R = 0.5 μm radius a magnetic field of 480 Tesla or at a distance r > R from the beam center

$$B_{\phi}(\text{Tesla}) = 480\ (R/r) \qquad (7.1)$$

This is such an enormous field (equal to the electrostatic attraction of the electron and positron beam) that we will detect a mutual deflection of the beams while they are still well separated. The force on a particle in one beam due to both the electric and the magnetic field of

the other beam is given in Gaussian units by

$$F = \frac{4e}{c}\frac{\hat{i}}{r} \qquad r \geq R \tag{7.2}$$

where $\hat{i} = e\,Nc/s$ is the peak current and s half the bunch length. The equation of motion therefore is

$$r'' + k\frac{1}{r} = 0 \qquad r \geq R \tag{7.3}$$

where $k = 4r_e N/\gamma s$ and r_e the classical electron radius. This differential equation can be solved by a Taylor series which up to 4th order is given by ($r_o' = 0$)

$$r(s) = r_o - \frac{1}{2}k\frac{s^2}{r_o} - \frac{1}{4!}k^2\frac{s^4}{r_o^3} + 0(6) \tag{7.4}$$

Finally we get for the deflection angle of one beam due to the other beam.

$$r'(s) \approx -k\frac{s}{r_o}\left(1 + \frac{1}{6}k\frac{s^2}{r_o^2}-\right) \tag{7.5}$$

This equation is a good approximation as long as the second term in the bracket is smaller than 1. In Fig. 14 this deflection angle is shown as a function of beam separation using the parameters of our design example (Table 2.1). At a separation of $r_o = 10$ μm we still have a deflection angle which in the horizontal plane is equal and in the vertical plane is seven times bigger than the internal divergence of the particles in the beam. By using monitors which detect deflections of the beam we can "see" the other beam even at large separation. In short we can say the beam of our model collider has an effective beam diameter of 5 to 10 μm even so the actual diameter is much smaller.

The required beam position stablilty of 5 to 10 μm still requires a sophisticated beam control system. However, as experience at SLAC has shown, this is the stability one can reach with present day technology.

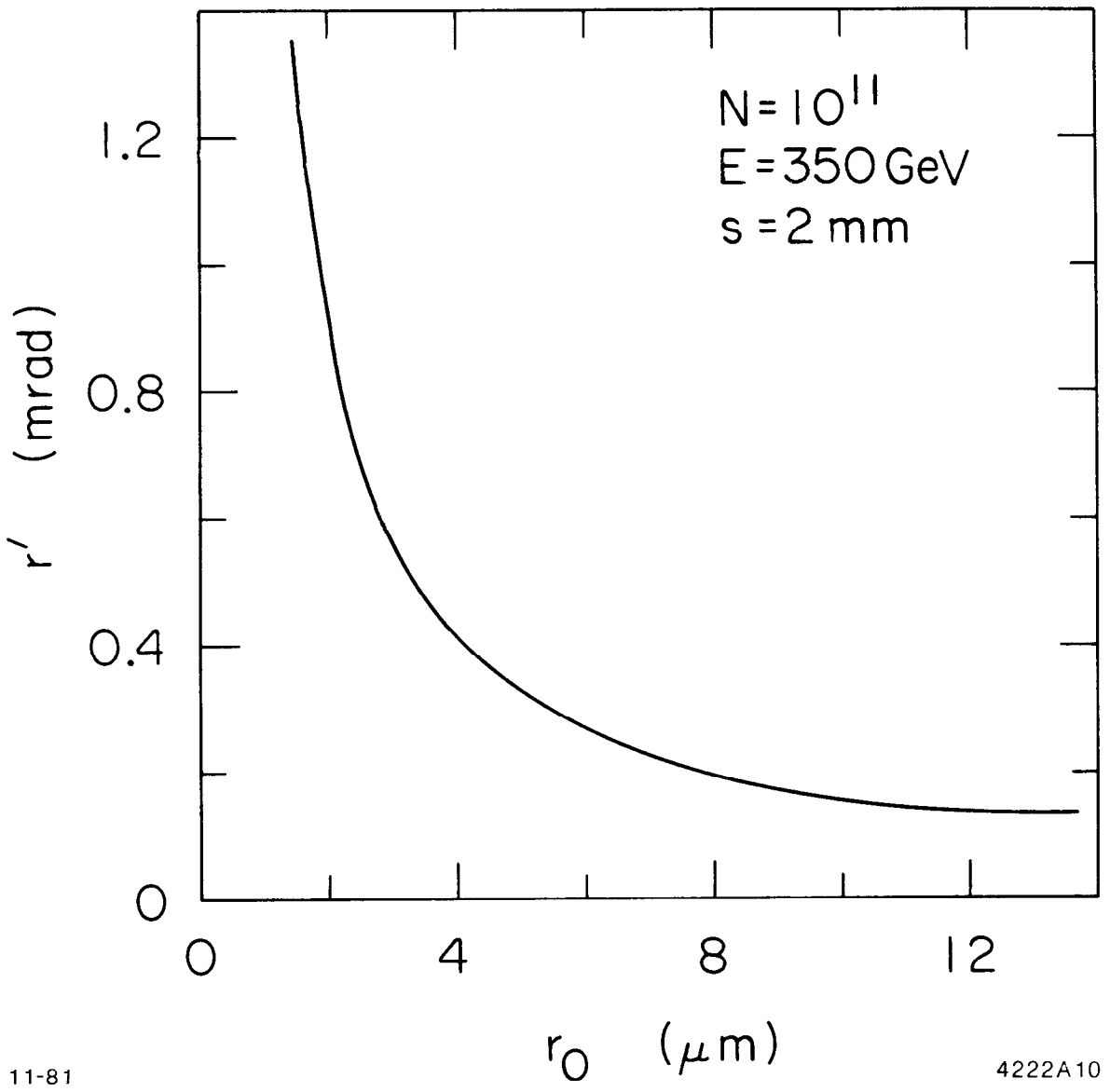

Fig. 14: Beam Beam Deflection as a Function of Beam Separation

As the beams collide head on and on center the electromagnetic fields of each beam make themselves noticable in still another way. They act as a focusing lens on the other beam. If the focal length of this focusing field is comparable to the bunch length we get a further compression of the beam cross section, called the "pinch effect". This effect has been thoroughly studied[44)45)] and can be parametrized by the disruption parameter D which we have defined already in Section 2. The action of the pinch effect is best demonstrated in Fig. 15 which shows two bunches colliding.[45)] This is a computer simulation which show clearly an enhancement in the particle density as the two bunches completely overlap. After the bunches have collided they disperse at a larger angle than they would do without the pinch effect. Since this beam beam focusing is a nonlinear effect we find the beam emittance after the collision largely diluted and the beams are not useful any more for further collisions. However, the emittance still is small enough to use the beam for fixed target experiments and/or positron production. The increase in luminosity due to the pinch effect is shown in Fig. 16.[45)] We see that an increase of as much as a factor 6 in luminosity is possible for a disruption parameter of $D \approx 4$. For higher disruption parameters no further enhancement in luminosity is realized. This is understandable noting that the disruption parameter D is related to the number n of transverse oscillations a particle performs during interaction with the other beam by:

$$D \approx 10\ n^2 \qquad (7.6)$$

A disruption parameter of D = 4 therefore translates to about 0.6 oscillations. Since the minimum spot size occurs after 1/2 oscillation we see that .6 oscillation covers all the tight beam region. An increase of D would not decrease the effective spot size any more. At large values of D the

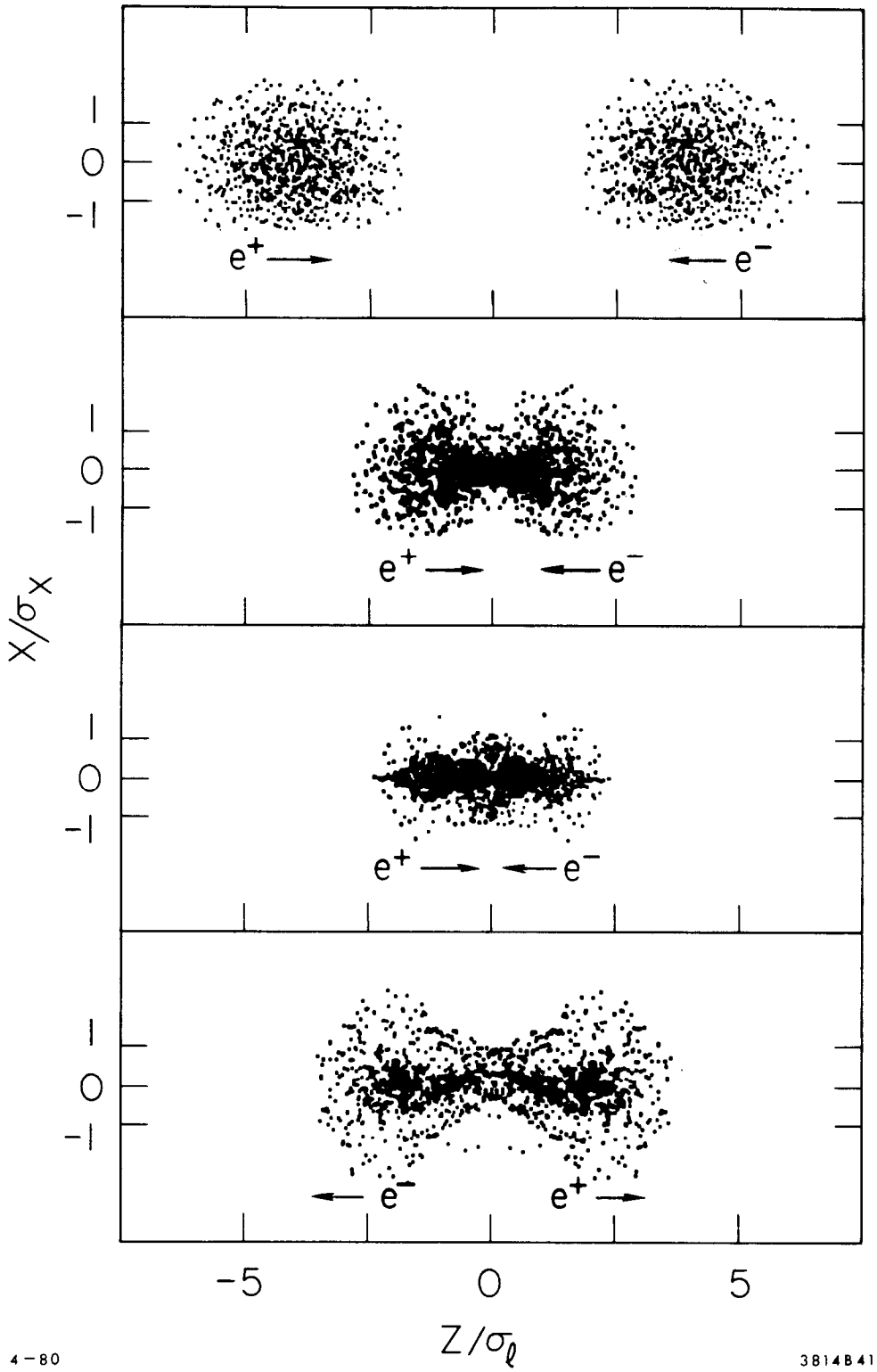

Fig. 15: Pinch Effect (Result of Particle Tracking)[45)]

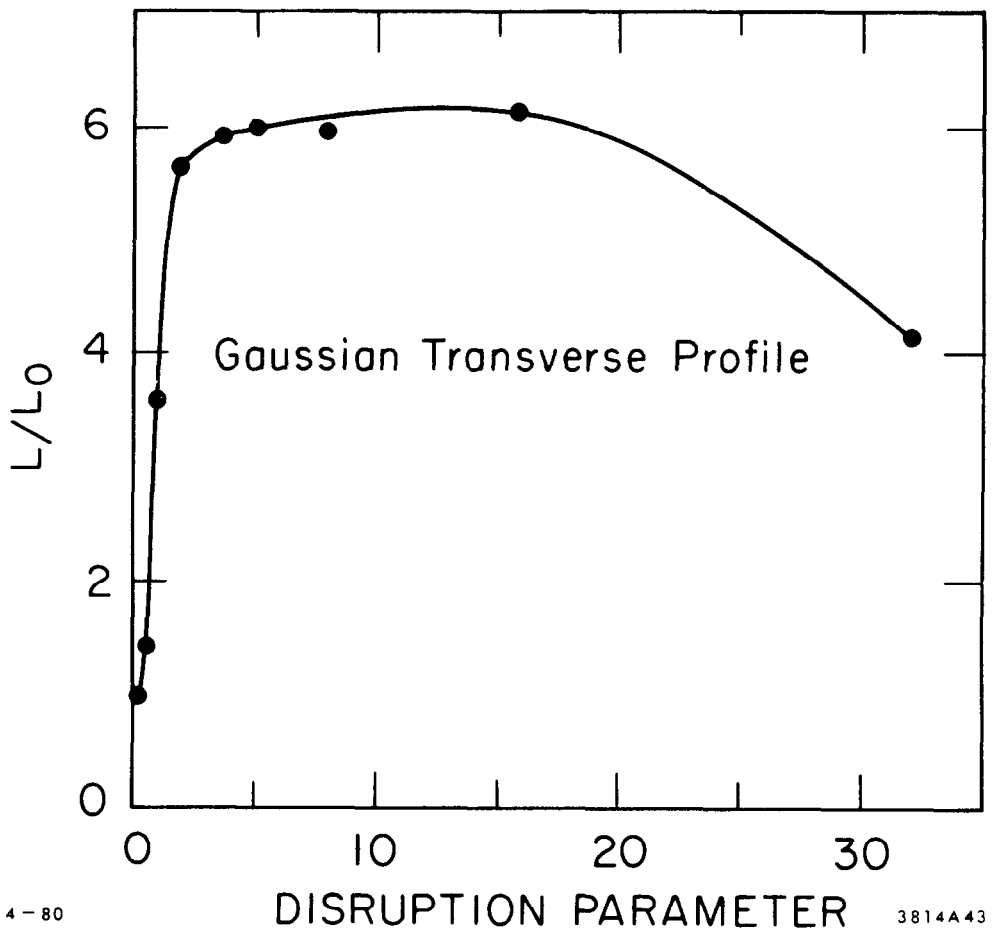

Fig. 16: Luminosity Enhancement as a Function of Disruption Parameter[45)]

luminosity is reduced again due to plasma instabilities. In a linear colliding beam facility, however, we do not want to go to a higher disruption parameter than 5 to 10 since the energyspread due to beam strahlung gets too large ($\Delta E/E \sim D^2$).

8. THE SLAC-LINAC-COLLIDER (SLC) PROJECT[7)]

8.1 General Description

The SLC project is a variant of a linear collider in as far as it uses only one linear accelerator. Both the electron and the positron bunch are accelerated in the same linac rf-pulse. At the end of the linac both beams are separated and travel through long arcs till they aim at each other. There a final focus system will compress the transverse size of the beams at the collision point to a radius of about 2 micrometer (Fig. 17).

The luminosity of the linear collider is given by:

$$\mathscr{L} = \frac{N^+ N^- \nu_{rep}}{4\pi\sigma^2} \qquad (8.1)$$

where we have set R = 1. (Compare with Eq. 2.1). With the present performance parameters of the Stanford Linear Accelerator we could expect a luminosity of no more than about $10^{24} cm^{-2} sec^{-1}$ apart from the fact that the beam energy would be only 30 GeV. The SLC project, to be feassible for high energy physics, requires therefore a significant upgrading of the linac beam parameters in energy, intensity and beam emittance (Table 8.1). The higher energy requires some modification of the klystron modulator while the intensity of the beams can be drastically increased only by a completely new design of the electron gun as well as the positron source. The required small beam emittance is achieved by two damping rings where the beams are stored for a few milliseconds to reduce the beam emittance through synchrotron radiation. A more detailed description of the new components will follow later in this report.

Table 8.1

	SLAC now	For SLC
energy (GeV)	30	50
intensity/S-band bunch	e^+ e^-	e^+/e^-
	10^8 10^9	$5 \cdot 10^{10}$
beam emittance ψ(m)	$6 \cdot 10^{-3}$ $6 \cdot 10^{-4}$	$3 \cdot 10^{-5}$

A schematic layout of the SLC facility is shown in Fig. 17 and the operation cycle goes as follows. The cycle begins just before the pulsing of the linac. The electron and positron damping rings each contain two bunches of 5×10^{10} particles at an energy of about 1.2 GeV. One of the positron bunches is extracted from the damping ring, passes through a pulse compressor which reduces the bunch length from two centimeters in the storage ring to less than one millimeter required for the linac, and is then injected into the linac. Both electron bunches are extracted from the electron damping ring, pass through an independent pulse compressor, and are injected into the linac behind the positron bunch. The spacing between bunches is 17.8 meters in the linac.

The three bunches are then accelerated down the linac. At the two-thirds points, the trailing electron bunch is extracted from the linac with a pulsed magnet and directed onto a positron-production target. The positron bunch and the remaining electron bunch continue to the end of the linac, where they reach an energy of 50 GeV. At the end of the linac the two opposite charge bunches are separated into the two arcs after which they pass through an achromatic matching and focusing section to collide head on with the opposite beam.

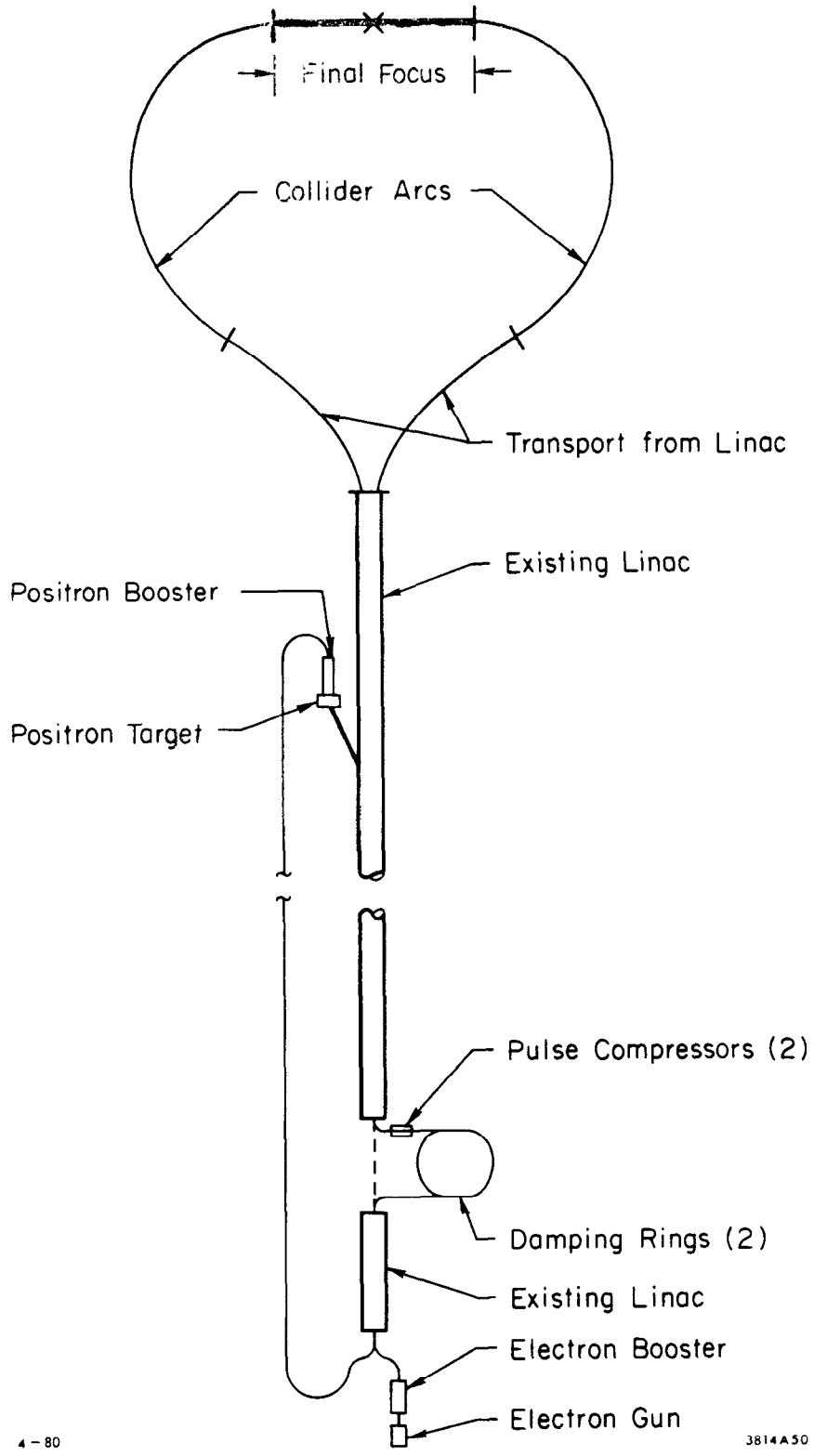

Fig. 17: Schematic Layout of the SLC Project

The positron produced by the "scavenger" electron bunch that was extracted at the two-thirds point of the linac pass through a focusing system at the positron source, a 200 MeV linear accelerator booster, a 180^{o} bend, and an evacuated transport pipe located in the existing linac tunnel to bring the positron bunch back to the beginning of the linac. At this point, the positrons pass through another 180^{o} bend and are boosted to an energy of 1.2 GeV in the first sector of the existing linac and then injected into the damping ring.

8.2 New Components for the SLC Project

Modification of the Klystron Modulator. In order to get a higher energy in the linear accelerator the second stage of the SLED rf-pulse compression system (SLED II)[10] will be installed. In the SLED principle the amplitude of the rf-pulse is increased at the expense of the pulse length. The maximum energy we expect to reach in this way is 51.6 GeV.

Electron Source. $5 \cdot 10^{10}$ or more electrons must be produced into a small emittance and captured into a single S-band bucket. Both a thermionic gun[23] or a photoemission gun can be used.[22] The latter utilizes a powerful frequency doubled, actively mode locked, Q-switched Nd: YAG laser to produce the electrons by photoemission from a semiconductor cathode. Such a gun has been used successfully at SLAC to provide polarized beams for the recent parity violation experiment.[25]

Positron Source.[7] Since we need as many positrons as we have electrons per bunch we are faced with the problem of producing one useful positron for every electron that strikes the convertion target. Fortunately the positron production is proportional to the energy of the electron. We accelerate therefore an electron bunch up to 33 GeV. At this point the

electron bunch gets directed to a tungsten-rhenium target to produce positrons. A series of pulsed and dc-solenoids between 100 kG and 5 kG capture positrons between 2 and 20 MeV at an emittance of 5 MeV mm. The effective yield is calculated at 4.8 positrons for each electron. This is far more than we need but it seems prudent to allow for considerable losses between the target and the damping ring.

Damping Rings and Bunch Compressor.[46] Two damping rings are required since both electrons and positrons cannot be produced with the required small emittance and high intensity. Some of the parameters of the damping rings are compiled in Table 8.2.

Table 8.2
Damping Ring Parameters

energy	E	=	1.21 GeV
intensity	N	=	$5 \cdot 10^{10}$ particles/bunch or
	I	=	68 ma/bunch
no. of bunches	n	=	2
circumference	C	=	35.27 m
tunes	ν_x/ν_y	=	7.23/2.78
damping time	$\tau_{x,y}$	=	3.06 msec
equilibrium beam emittance	$\varepsilon_x=\varepsilon_y$	=	$9 \cdot 10^{-9}$ rad m

In order to achieve fast damping we have to utilize high bending fields (2 Tesla) and to obtain a small emittance the focusing has to be very strong (63 T/m).[6] We need for the electrons a damping time of one inter linac pulse interval of 5.6 msec and twice that much for positrons. Therefore,

every 5.6 msec there are 2 electron bunches and one positron bunch ready to be accelerated in the linac. One of the electron bunches will be used for positron production and the other electron bunch and the positron bunch are accelerated to 50 GeV for collision.

The damping of the bunches introduces a slight complication. Particle bunches in storage rings are of the order of 2 cm long. This is too long a bunch for an S-band linear accelerator. Between the damping ring and the linear accelerator, we therefore have a bunch compressor system. This system compresses the bunch length to 1 mm at the expense of the energy spread as described in Section 1.

Linac Control System. The acceleration of $5 \cdot 10^{10}$ particles in one S-band bucket in SLAC is at this time not feasible. The interaction of a bunch of this intensity (I_{peak} = 1200 amps) with the accelerator structure generate wake fields which act back on the bunch in a destructure way. There are two components of the wake field. The longitudinal component generated by the head of the bunch decelerates the tail of the bunch causing a large energy spread. This effect we can counteract by accelerating the bunch ahead of the crest of the rf-wave. In this way the tail gets accelerated more than the head and if we now add the deceleration of the tail due to the wake field we can minimize the energy spread at the end of the linac. An energy spread of less than 1% seems to be possible (Fig. 18).[7)]

If the head of a bunch travels off center through an accelerating structure a transverse wake field is generated. This field acts back on the tail of the bunch in such a way as to increase the deviation from the center. Therefore, a straight bunch changes more and more to a "banana" shape during acceleration till the tail gets scraped off. This is called the beam break-up phenomenon. Clearly the effect is enhanced proportional to the charge in the bunch. For a given charge in the bunch this beam

break-up can be minimized by improving the focusing, the control of the trajectory in the accelerator and the alignment of the accelerator. A major upgrading of the SLAC control system is required to make the SLC project a viable project. With the new control system calculations show that for a bunch population of $5 \cdot 10^{10}$ the emittance growth due to the "banana" effect is not more than 15% assuming an alignment tolerance of 0.1 mm for the focusing elements and the accelerating structures. With some optimism and operating experience it might be possible later to increase the intensity to about $7 \cdot 10^{10}$ particles per bunch.

Arc Beam Transport and Final Focus. After acceleration to 50 GeV the two bunches are split and travel through two half circles toward the collision point. Special precaution has to be taken to minimize the increase of the beam emittance due to synchrotron radiation in the arc magnets. The growth in the beam emittance is given by

$$\Delta\varepsilon \text{ (rad m)} = 2.1 \cdot 10^{-11} \rho\phi \langle \mathcal{H}/\rho^3 \rangle E^5$$

where ρ(m) is the bending radius, ϕ(rad) the total bending angle of the arc, $\rho \cdot \phi$ the length of the arc, E(GeV) the energy and $\langle \mathcal{H}/\rho^3 \rangle$ a quantity which depends on the focusing and the bending radius. Since $\langle \mathcal{H}/\rho^3 \rangle \sim \rho^{-5}$ it is clear that the arcs should be as large as the available site allows them to be. The focusing is chosen to be very strong to get a betatron phase advance of 108° per cell which gives an almost minimum emittance growth.[47] With these parameters in mind it turns out impossible to design a separated function lattice which would not destroy the small beam emittance coming from the linac. We chose therefore a combined function magnet with a cross section as shown in Fig. 19. Each arc has some 500 magnets each 2.6 m long with every second magnet rotated by 180° about the

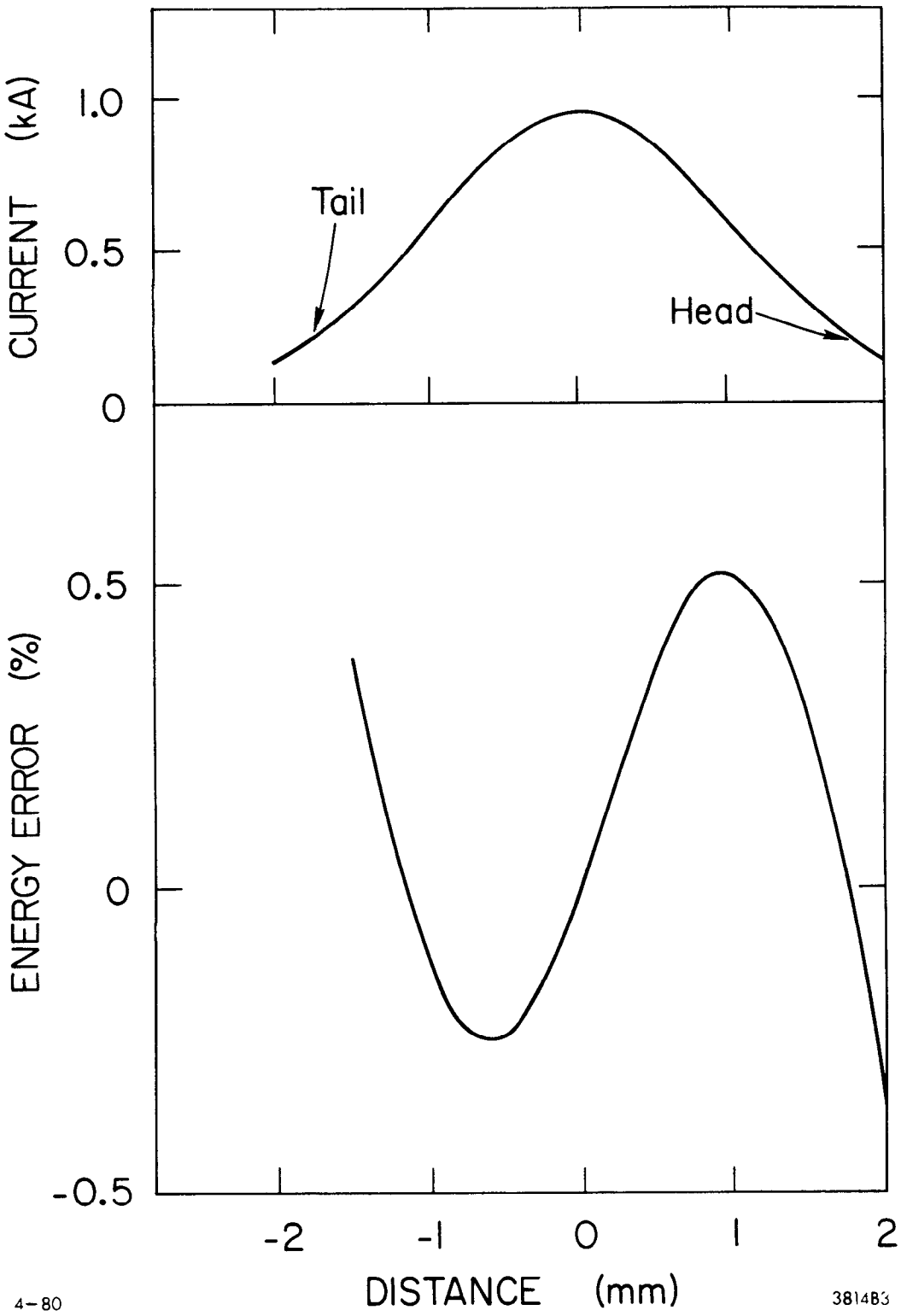

Fig. 18: Energy Spread in the SLC Beams[7)]

Figure Captions

Fig. 1: Schematic Layout of a Colliding Beam Facility

Fig. 2: Damping Ring Scaling

Fig. 3: Bunch Length Compressor

Fig. 4: "Jungle Gym" Accelerating Structure[17)]

Fig. 5: Photon Energy and Pair Production Cross Section

Fig. 6: Positron Production Efficiency

Fig. 7: Polarization Rotators

Fig. 8: Wake Fields for a Parallel Plate "Cavity"[38)]

Fig. 9: Longitudinal Wake Field per Cell for the SLAC Structure[7)]

Fig. 10: Transverse Wake Field per Cell for the SLAC Structure[7)]

Fig. 11: Principle of the Correction of Chromatic Errors

Fig. 12: Cause of Geometric Aberrations

Fig. 13: Beam Spot Size at the Collision Point (Result of Particle Tracking)[45)]

Fig. 14: Beam Beam Deflection as a Function of Beam Separation

Fig. 15: Pinch Effect (Result of Particle Tracking)[45)]

Fig. 16: Luminosity Enhancement as a Function of Disruption Parameter[45)]

Fig. 17: Schematic Layout of the SLC Project

Fig. 18: Energy Spread in the SLC Beams[7)]

Fig. 19: Magnet Cross Section for the SLC Arc[7)]

Fig. 20: Luminosity as a Function of the Center of Mass Energy

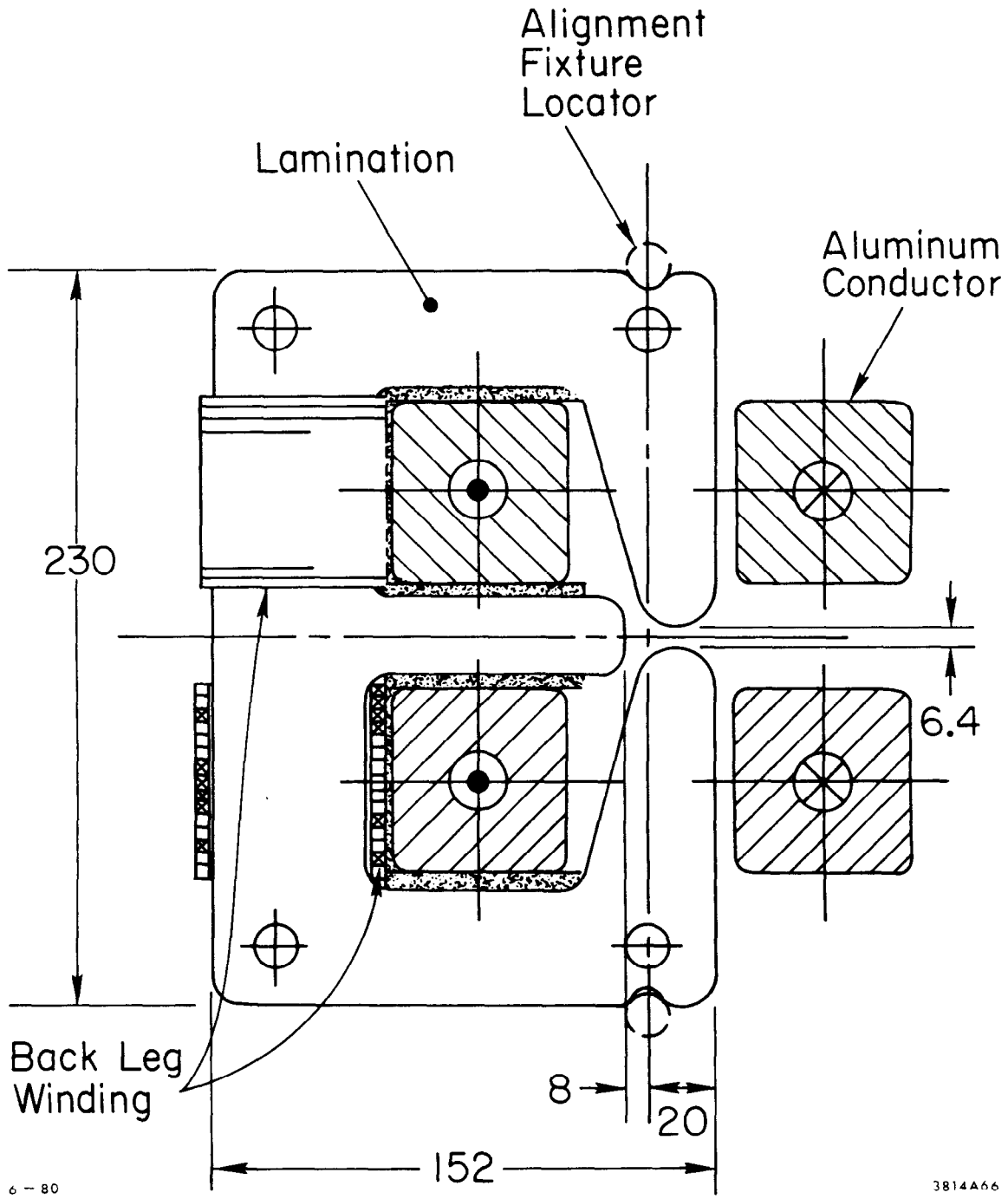

Fig. 19: Magnet Cross Section for the SLC Arc[7)]

beam axis with respect to the orientation of the magnet in Fig. 19. This way one cross section serves for both the focusing and the defocusing magnet. All magnets are strung like beads on four aluminum conductors which serve as the excitation coils.

At the ends of the arc the beam enters a 100 m long final focusing system which compresses the typical beam size of 30 μm in the arcs to about 2 μm at the interaction point.[43] Since the energy spread in the beam is about ± 0.5% we face severe chromatic image errors in the final focus system. A sophisticated final focus system was worked out to both minimize the chromatic and geometric (astigmatism etc.) errors in the beam spot size at the collision point. A ray tracing study confirmed the feasibility of the design of the final focus system.[43] In Fig. 13 the result of the ray tracing calculations shows 50% of the beam within a radius of 2μ and 90% within 4 μm which is what we assumed as a design goal.

8.3 Luminosity and Improvements

At the collision point we expect the $5 \cdot 10^{10}$ particles per bunch to have a gaussian distribution with a standard value for the beam radius of σ = 2 μm at 50 GeV. Since the pulse repetition rate is ν_{rep} = 180 sec^{-1} we calculate from Eq. (8.1) a luminosity of

$$\mathscr{L}_o = 1 \times 10^{30} cm^{-2} sec^{-1} \text{ at } 50 \text{ GeV}. \qquad (3)$$

For other energies the luminosity is shown in Fig. 20.[7] This luminosity calculation does not take into account an enhancement due to the pinch effect. At low energies the luminosity increases with energy since adiabatic damping during acceleration in the linac reduces the beam emittance. At energies above 60 GeV per beam, however, the emittance blow-up in the arcs becomes dominant and reduces the luminosity again.

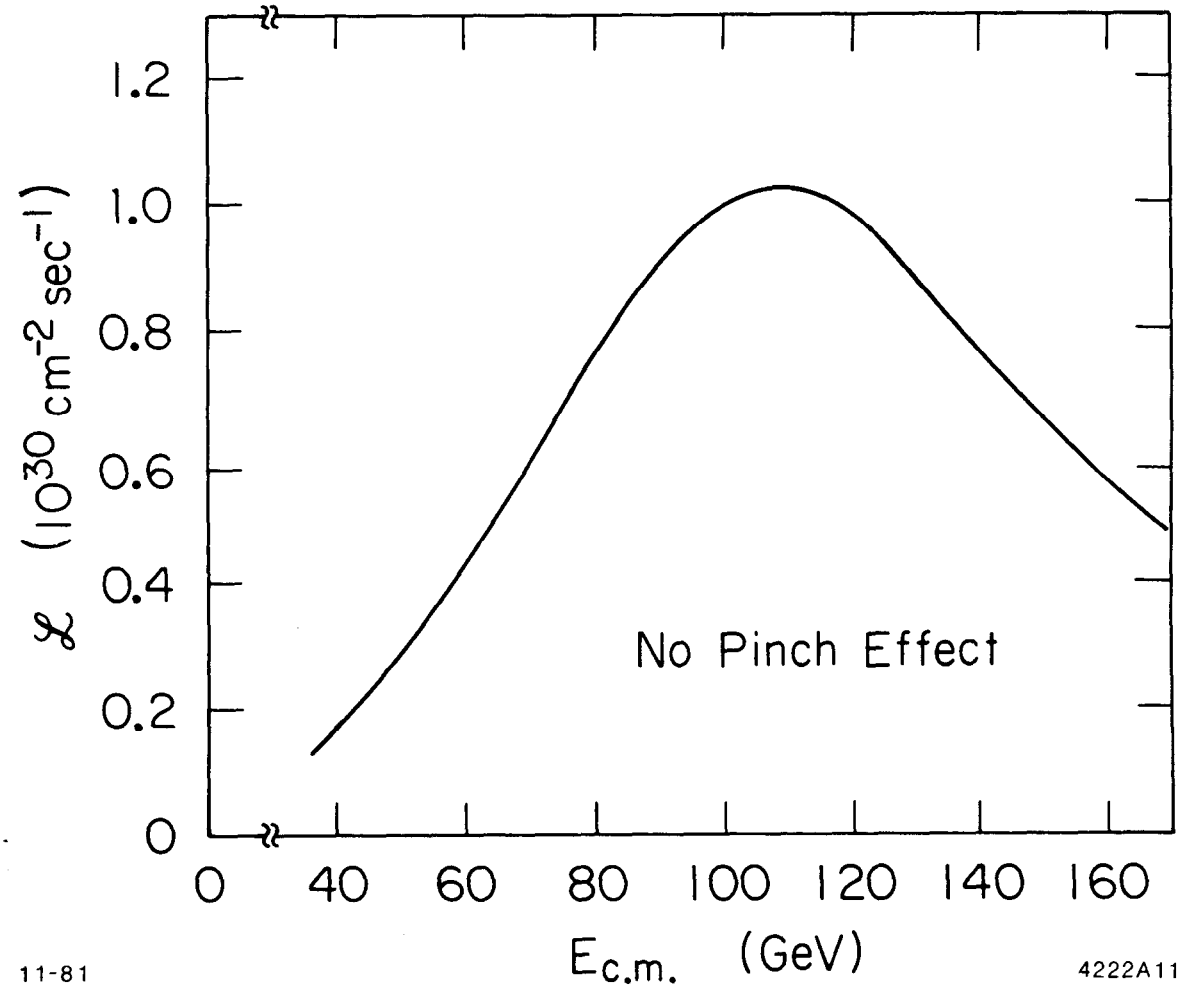

Fig. 20: Luminosity as a Function of the Center of Mass Energy

A good prediction of the luminosity in storage rings always has been very difficult because it is still not known which parameters cause the beam-beam effect to limit the luminosity at a certain level. We think that a much safer prediction of the luminosity can be made for a colliding linac beam facility. Unlike in a storage ring here the beams meet only once and are disposed of after the collision. We, therefore, believe we can calculate what actually happens when both beam collide.

One possibility for improvement, which is evolutionary, is to attain more precise control of the trajectory in the linac. This would allow an increase in the number of particles to maybe $7 \cdot 10^{10}$ per bunch before exciting serious emittance growth from transverse wakefields.

Another possibility is being actively pursued at SLAC right now. This is to reduce the beam spot size at the collision point further to about 1.3 μm. In order still to control the chromatic and geometric errors we plan to use for the last quadrupoles on either side of the collision point permanent magnets made from a cobalt samarium alloy ($SmCo_5$).[48] Such magnets have permeability of $\mu = 1$ and can therefore be moved into the detectors without perturbing the detector fields. A small sample quadrupole has been found suitable and a full size prototype is being built soon. If both improvement possibilities should be realized we could expect a luminosity of $4.7 \cdot 10^{30} cm^{-3} sec^{-1}$ without enhancement due to the pinch effect and $\mathscr{L} = 2.3 \cdot 10^{31} cm^{-2} sec^{-1}$ if we include the pinch effect.

For the SLC project we plan to use a laser driven photo emission gun to produce an intense beam of longitudinally polarized electrons.[22)25)] The polarization was 50%[25)] and with the new electron gun[22)] a polarization

of 90% seems possible. We see no possibility to also produce polarized positrons. As we have seen in Section 5 the energy of the SLC is too low to produce positrons by the use of wiggler generated circularly polarized photons.

The longitudinally polarized electron beam is accelerated to 1.21 GeV. In the transport system from the linac to the damping ring a proper combination of vertical magnetic fields and a 6 Tm superconducting solenoid will cause a g-2 precession such as to erect the electron spin into the vertical direction.[35] This direction of the spin will be preserved during the storage time in the damping ring. In the transport line from the damping ring to the linac we have two 6 Tm superconducting solenoids together with the necessary vertical magnetic fields. Depending on the setting of the strength of these two solenoids we can produce any spin direction we want at the reentry point to the linac. In practice this spin direction will be chosen such that together with the g-2 precession in the collider arcs we obtain the desired polarization (longitudinal or transverse) at the collision point (Fig. 7).

8.4 Conclusion

The SLC is designed to be a pioneer project for a new kind of a colliding electron positron beam facility. It serves two purposes, first to provide a center-of-mass energy at the collision point of 100 GeV to allow the exploration of an extremely interesting area in high energy physics, second to test the feasibility and special features of still larger linear colliding beam facilities.

Critical questions for such a facility can be answered from the operation of the SLC, like what are the maximum charges per bunch that can be generated and accelerated in a linear accelerator, what is the minimum

beam emittance achievable, is our present knowledge on the final focus system sufficient, can we use permanent magnet quadrupoles and does the pinch effect work in our favor.

Since the electron storage ring technique is reaching its limits, new avenues in accelerator physics have to be pursued and building the SLC is the first step in this direction.

REFERENCES

1) J. E. Augustin, N. Dikanski, Y. Derbenev, J. Rees, B. Richter, A Skrinski, M. Tigner, H. Wiedemann, Proc. of the Workshop on Possibilities and Limitations of Accelerators and Detectors FNAL (1979) p. 87.

2) Design Study for a 22 to 130 GeV e^+e^- Colliding Beam Machine (LEP) CERN/ISR-LEP/79-33 (1979).

3) M. Tigner, Nuovo Cimento 37, (1965) 1228.

4) J. R. Rees, IEEE Vol. NS-28, No. 3 (1981) 1989.

5) M. Sands in Physics with Intersecting Storage Rings 1971 Academic Press. Ed. B. Touschek.

6) H. Wiedemann, 11th Int. Conf. on High Energy Accelerator 1980 Birkhauser Verlag, Basel p. 693 or SLAC-PUB-2537 (1980).

7) SLAC-LINEAR-COLLIDER, Conceptual Design Report (1981), SLAC-229.

8) M. Bassetti, M. Gygi-Hanney, LEP-NOTE-221, CERN Geneva, 1980 (internal note).

9) E. D. Courant and H. S. Snyder Ann. of Phys. 3, 1-48 (1958).

10) Z. D. Farkas et.al. Proc. of the IXth Int. Conf. on High Energy Accelerators, Stanford, CA 1974 p. 576.

11) U. Amaldi Proc. Int. Sym. on Lepton and Photon Interactions at High Energies FNAL, Batavia, (1979).

12) H. Gerke, K. G. Steffen DESY-PET 79/04 (1979) (internal note).

13) A. Citron et.al. NIM 164 (1979).

14) H. Lengeler LEP-210 (1980) CERN, Geneva (internal note).

15) The Stanford 2-Mile Linear Accelerator ed. by R. B. Neal (1968). Benjamin, New York.

16) P. B. Wilson IEEE NS-26 No. 3 (1979) 3255.

17) P. B. Wilson IEEE NS-23 No. 3 (1981) 2742.

18) R. A. Alvarez et.al. Particle Accelerators Vol. 11 (1981) 125.

19) B. Zotter, K. Bane PEP-Note-308 (1979) SLAC (internal note).

20) Proc. of the 2nd ICFA Workshop on Possibilities and Limitations of Accelerators and Detectors, Les Diablerets (CERN) 1979.

21) V. E. Balakin et.al. Proc. of the 6th All Union Accel. Conf. (1979) Dubna.

22) C. Sinclair, R. Miller IEEE NS-28, No. 3, (1981) 2649.

23) R. Koontz et.al. IEEE NS-28, No. 3, (1981) 2213.

24) R. Miller private communication.

25) C. Y. Prescott et.al. Phys. Lett. 77B, 347 (1978); M. J. Alguard et.al. IEEE, Vol. NS-24, No. 3, (1977) p. 1603.

26) Linear Accelerators ed. by P. M. Lapostolle and A. L. Septier, North Holland Pub. Co. Amsterdam (1970).

27) V.E. Balakin, A. A. Mikhailichenko Preprint INT 79-85 (1979), Novosibirsk.

28) U. Amaldi Proc. of the 2nd ICFA Workshop on Possibilities and Limitations of Accelerators and Detectors Les Diablerets (1979) p. 21.

29) B. M. Kincaid J. of Appl. Physics, Vol. 48, No. 7 (1977) 2684.

30) E. M. Purcell SSRP Report No. 77/05 ed. by H. Winick and T. Knight (1977) Stanford University.

31) C. Bazin et.al. J. Physique - Letters 41 (1980) L-547.

32) W. Heitler, The Quantum Theory of Radiation Oxford, University Press.

33) K. Halbach LBL-11393 Berkeley (1980) and Proc. of the Int. Conf. on Charged Particle Optics, Giessen, W-Germany (1980).

34) H. Olsen, L. C. Maximon Phys. Rev. Vol. 114, No. 3 (1959) 887.

35) R. Stiening AATF/80-28 SLAC (1980) unpublished.

36) H. Weyl J. Math. 143, 177 (1913).

37) E. N. Condon J. of Appl. Physics Vol. 12 (1941) 129.

38) A. W. Chao, P. L. Morton PEP-105 SLAC (1975) (internal note).

39) R. F. Koontz et.al. IEEE NS-24, 1493 (1977).

40) E. V. Farinholj et.al. VIth Int. Conf. on High Energy Accelerators, Cambridge 1967 CEAL-2000.

41) A. W. Chao, B. Richter, C. Y. Yao, 11th Int. Conf. on High Energy Accelerators CERN, Geneva (1980) Birkhauser Verlag, Basel p. 597.

42) K. L. Brown, R. Servranckx, 11th Int. Conf. on High Energy Accelerators CERN, Geneva (1980) Birkhauser Verlag, Basel (p. 656).

43) K. L. Brown, J. E. Spencer IEEE Vol. NS-28, No. 3, 2568 (1981).

44) R. C. Sah, 11th Int. Conf. on High Energy Accelerators CERN, Geneva (1980) Birkhauser Verlag, Basel (p. 736).

45) R. Hollebeek NIM 184 (1981) 333.

46) H. Wiedemann AATF/79/8 and ATTF/79/11 internal notes SLAC (1979).

47) R. Helm, H. Wiedemann PEP-Note-303 SLAC (internal note)
H. Wiedemann NIM 172, 33 (1980).

48) R. F. Holsinger Proc. of the Proton Linear Accelerator Conference Brookhaven (1979).